An Enhanced State Estimator for Bad Data Detection using PMU Measurements

By

Abubeker Alamin

A Thesis Presented to the Masdar Institute of Science and Technology in Partial Fulfillment of the Requirements for the Degree of

Master of Science

In

Electrical Power Engineering

An Enhanced State Estimator for Bad Data Detection using PMU Measurements

By

Abubeker Alamin

A Thesis Presented to the Masdar Institute of Science and Technology in Partial Fulfillment of the Requirements for the Degree of

Master of Science in Electrical Power Engineering

May 2015

AUTHOR'S DECLARATION

I understand that copyright in my thesis is transferred to Masdar Institute of Science and Technology.

Author ____________________________________

RESEARCH SUPERVISORY COMMITTEE MEMBERS

Dr. Jimmy Peng, Chair, ____

Masdar Institute of Science and Technology

Dr. Amer Al Hinai, ____

Masdar Institute of Science and Technology

Dr. Seddik M. Djouadi ____

Masdar Institute of Science and Technology

Abstract

The deployment of phasor measurement units (PMUs) by power electric utilities to enhance the operating capabilities of state estimators is an emerging trend around the world. In the literature, several publications introduced PMU measurements into the current state estimators to boost their estimation accuracy. However, they could not replace all the existing conventional measurements due to their high cost. Instead, PMUs are being deployed gradually in few numbers by many utilities. One of the essential functions of a state estimator that could potentially benefit from PMU technology is bad data detection and identification. Bad data are gross errors coming from flawed measurement devices and has the potential to affect the estimation results leading to incorrect information of the system status. Therefore, state estimators are required to be equipped with advanced bad data detection techniques. One of the most commonly used bad data detection techniques is the largest normalized residual test (LNRT). However, it is known to fail with certain measurements known as critical measurements.

In this thesis, a state estimator (SE) based on weighted least squares (WLS) was developed and evaluated against Iterative Kalman Filter (IEKF). For bad data detection, largest normalized residual test (LNRT) was integrated into the WLS estimator, and a detailed analysis of its detection threshold was evaluated. Finally, the LNRT capability was enhanced by incorporating PMU measurements at certain locations to enable it to detect bad data within critical measurements. An IEEE 14 Bus test system was simulated in Matlab under various scenarios. The results demonstrated the enhancement of LNRT detection capability by introducing few PMUs into the system and strategically placing them to eliminate critical measurements. This made LNRT detect and identify any bad data irrespective of its location. Moreover, variation of the value of detection threshold with redundancy ratio dictating against fixing the threshold was observed. Generally,

the proposed technique showed an improvement on the bad data detection capability and state estimation results accuracy.

This research was supported by the Government of Abu Dhabi to help fulfill the vision of the late President Sheikh Zayed Bin Sultan Al Nahyan for sustainable development and empowerment of the UAE and humankind.

Acknowledgments

I would like to thank my advisor Dr. Jimmy Peng for his great support and efforts during past two years. I really appreciate the time and effort he spent with me to enhance my technical and academic attitude. I would also like to appreciate for the continuous support on successful accomplishment of this thesis. Dr. Haris has also been a great support on the research. Moreover, I would like to extend my gratitude to thank the entire Electrical Power Engineering (EPE) department faculty, Dr. Hatem Zeineldin, Dr. Weidong M. Xiao, Dr. Vinod Khadkikar, Dr. Amer Al Hinai, Dr. Mohammed Shawky, Dr. Seddik M. Djouadi and Dr. Jimmy Peng. I would like to thank all Masdar faculties who instructed courses professionally during my master program. Great thanks to our research group Salish Maharjan, Younes Isbeih and Maksymilian Klimontowicz and my friends in Masdar Institute Jim, Jamrus, Desmond and Isaac whom I am proud of all the memories I have with. I would also like thank my friend Yohannes Gidey.

Most importantly, I want to thank ALLAH who blessed me with faith and patience and guiding me to important path of my life and made this happen, and my parents Jemal Alamin and Sofia Mohammedsiraj who raised me and educated me so that I am able to join this world class institute.

Contents

CHAPTER 1

Introduction

One of the key aspects to maintain the reliability of a large system such as the electric power grid is to provide feedback information to the control centers. Finding a way to accurately monitor the system has been the goal of power engineers for many years. If system operators can be provided with appropriate information regarding the conditions of the grid, they can make decisions that will improve not only the reliability of the system but also to plan more effectively for the future.

State estimation (SE) is an outcome of electrical power engineering that evolved from these necessities. Ever since 1960's, engineers begun developing techniques that could help them monitor the power network from control centers. They developed system models that represent the system structure and developed communication systems to collect the measurements. A computer then took these information and computed a best likely representation of the system operating conditions. The results are regarded as the system states. According to the results, a trained professional could understand what may be happening in the grid in near real-time.

However, measurements could not always be trusted as even a single flawed measurement information could significantly alter the state estimation outcome and affect control decisions. In fact, a state estimator would not be a reliable application without its ability to detect and locate bad measurements. Therefore, to prevent such problems, engineers developed several techniques to assess the flawed measurements. Depending on the type of SE algorithm employed bad data detection process are executed either pre or post estimation.

In this thesis, the existing techniques and methodologies in the area of SE are reviewed and extended to enhance its robustness and reliability. This was done by improving the bad data detection capability and estimation accuracy of conventional state estimators by employing PMU measurements. The remainder of this Chapter presents the research motivation, research contributions, and thesis organization.

1.1 Motivations and Relevance to Masdar/UAE

Under the patronage of Abu Dhabi Government and directives for their master plan known as "Abu Dhabi Vision 2030", ADWEA is fully committed to achieve the target of getting 7% of its network load to be supplied through renewable resources by year 2020. Due to the intermittent nature of renewable energy resources, it is required to maintain a close monitoring and control of the system states in order to deliver a secure and reliable power to consumers because failure to do so may cause blackouts.

In order to achieve these objectives, it is crucial to accurately monitor the state of the power grid as the operating conditions continue to change during the daily operation. State estimation is therefore at the core of addressing the reliability of the power systems.

State estimators should also be equipped with robust detection strategies in order to allow them to remove bad data. To achieve this need, strategic utilization of installed Phasor Measurement Units (PMUs) could enhance the bad data detection capability while also improving the estimates. This is the primary motivation of the thesis.

1.2 Research Contributions

The main objectives of this thesis are to detect and eliminate bad data. This would ensure unbiased state estimations, which would facilitate proper execution of all other application functions that rely on state estimator outputs at the control center. However, despite having full observability, the system may have vulnerable areas that are called critical measurements. Errors in these measurements will not be detectable and poses a security concern. Therefore, one benefit of introducing redundant PMU measurements would be to let them transform these critical measurements into redundant ones. Thus, eliminating the vulnerability of critical measurements to bad data.

In Summary, this thesis contributed the following investigations:

- Detailed comparison of the estimation accuracy of Weighted Least Squares (WLS) against Iterative Kalman Filter (IEKF)
- Exhaustive evaluations of the impact of detection threshold in LNRT on improving bad data detection
- Incorporated PMUs into the estimator to improve LNRT effectiveness to detect bad data, and improve estimation accuracy as well

The findings showed decent performance with a few drawbacks that are envisioned in the future work of this research.

1.3 Thesis Organization

A literature review on the developments, existing techniques and methodologies in the area of state estimation are reviewed in chapter 2. The third chapter presents the mathematical formulation of the algorithm employed by traditional state estimation techniques. It presents system modeling, maximum likelihood estimation, weighted least squares estimation, and a brief discussion concerning the state estimator consisting of phasor and conventional measurements. The fourth chapter introduces various types of bad data and their impacts on the accuracy of SE. A mathematical model for bad data analysis is presented based on maximum normalized residual test. A comprehensive study of types of measurement and their effects on bad data is also discussed. The fifth chapter discusses the results of comparison between WLS and IEKF, investigation of detection threshold of LNRT, and improved LNRT capability using PMUs. Then chapter six presents the conclusions and future work of this thesis.

CHAPTER 2

Literature Review

Since the pioneering work of F.C. Schweppe in 1970 [1-3], SE has become an important function in supervisory control and planning of power grids. It helps monitor the state of the power grid, which is defined as the voltage magnitude and phase angle at each bus. SE lies at the heart of Energy Management Systems (EMS) which can perform various important control and planning tasks such as establishing near real-time network models, optimizing power flows, and bad data detection/analysis [4],[5, 6]. The EMS and supervisory control and data acquisition (SCADA) system are a set of computational tools used to monitor, control, and optimize the performance of a power system [7].

The relationship between SE and the SCADA system is shown in Fig.2.1. The SCADA system obtains measurements from metering devices like remote terminal units (RTUs) and, more recently, phasor measurement units (PMU). Based on the measurements and a known system model, the state estimator calculates the system states and provides the necessary information to the supervisory control, which then takes action accordingly [6].

The conventional SE is built into EMS and consists of four main processes as shown in Fig.2.1. The topology processor tracks the network topology and maintains a real-time database of the network model. Observability analysis is a process that is run to ensure if the measurement set is sufficient to perform SE. Finally, the bad-data processing identifies any gross errors in the

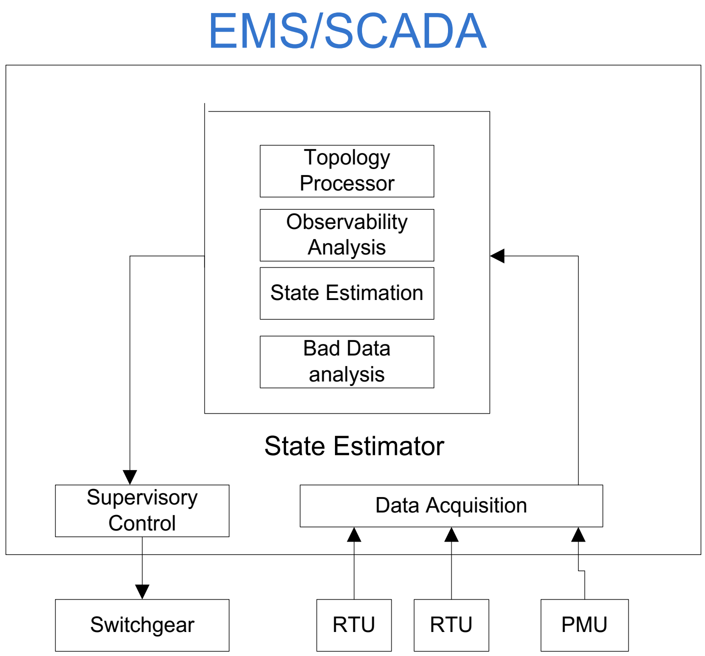

Fig. 2.1 Different elements of the EMS/SCADA

measurement set and eliminates bad measurements. Moreover, the developments of the observability and bad data analysis are discussed in detail in the next sections.

2.1 Overview of State Estimator Structure

2.1.1 State Estimation

Several methodologies in the areas of state estimations were developed over the past decades. Literature on the types of SE algorithms were presented in [5, 8-10]. SE also has different approaches based on application of the algorithms such as conventional SE [5], distributed SE or multi area SE (MASE) [11]. Depending on the timing and evolution of the estimates, SE schemes may be broadly classified into two basic distinct paradigms: static SE (SSE) and Dynamic SE (DSE) [6]. This section briefly discusses these two classification.

2.1.1.1 Static State Estimation

If states variables are calculated from measurement set of the same time instant, then such estimator is known as SSE. This process is then repeated at suitable intervals of time in order to constantly know the status of the grid. SSE are widely used in power systems, and play an important role for the reliable and secure operation of transmission and distribution systems. One of the most commonly used types of SSE in utilities is the weighted least squares (WLS) methodology [9]. It was formulated as an optimization problem with a notion of minimizing the squares of the differences between the measured and estimated values calculated using the corresponding power flow equations. The WLS uses the Newton-Raphson algorithm to obtain the state estimates. It is further explained in Chapter 3.

There have been numerous findings on different variations of WLS further to improve specific aspects of the algorithm. Fast Decoupled State Estimator [12, 13] is an example in which voltage magnitudes and phase angles are processed separately. The voltage magnitude values are concerned with the reactive power measurements while angles were related to active power measurements. Regularized Least Square for power systems in [14] proposed a type of WLS that was able to function in cases of partial observability. Another extension of SSE also included the Sequential SE which has the advantage of being able to perform updates with partial measurement set [15]. This enabled the method to address the problem of data loss and bad data. An SSE algorithm based on linear programming known as Least Absolute Value (LAV) was also developed in [16, 17].

Generally, under normal operating conditions, the power system is regarded as a quasi-static system that changes steadily but slowly [8]. Therefore, in order to continuously monitor the power system, state estimators must be executed at short intervals of time. But with the inherent expansion of power systems, with the increase of generations and loads, the system becomes extremely large for SE to be executed at short intervals of time since it requires heavy computation resources. Therefore, a technique known as Tracking SE [18, 19] was developed. Once state estimates were calculated, the method simply update the next instant of time using a new measurement set obtained for that instant, instead of again running the entire SSE algorithm. Tracking estimators help EMS to keep track of the continuously changing power system without actually having to execute the entire SE algorithm. This allows continuous monitoring with reasonable utilization of computing resources.

2.1.1.2 Dynamic State Estimation (DSE)

Although tracking is the simplest way of monitoring the changes, it does not include the physical modeling of the time behavior of the system [20]. This led for the development of DSE, where the physical model of the time-varying nature of the system would be considered. This type of algorithms has the advantage to predict the states of the system one-step ahead. Their forecasting ability provide advantages in performing security analysis and allows more time for the operator to take control actions [20]. However due to the mathematical modelling of the non-linearity of the system, DSE is computationally expensive and therefore is not widely implemented in the industry [21].

DSE algorithms consist of two steps known as the prediction and correction steps. The prediction of the state variables involves the modeling of the power system behavior and is calculated based on a mathematical model by considering the nonlinearities of the measurement functions [8]. The correction step acts like a filter to remove the measurement errors upon the arrival of measurements.

The Extended Kalman Filter (EKF) is the most widely used algorithm to perform DSE [22]. Other forms of kalman filters like Unscented Kalman Filter (UKF) [23], and Iterative EKF [24] were also proposed in the literature. Other algorithms used to perform DSEs include Artificial Neural networks (ANN) [25] and Fuzzy logic [26] which are also computationally complex. Generally DSEs are well suited when the dynamics of the power systems are smooth and follow the historical value. In other words, they could fail to accurately estimate when there exists a bigger changes in operating points. Hence, the SSE methodology is adopted in this thesis to fit the challenges stated previously.

The work presented in this thesis adopts the work presented in [1-3, 27], where SSE based on WLS is used. It is then cascaded with a linear post-processing step [28] to include PMU measurements and enhance the bad data analysis. A detailed investigation of the detection threshold was also conducted. The developments on bad data analysis are discussed in the next sections. The IEKF based on the works on [29-31] is also adopted to compare the performance of the WLS estimator.

2.1.2 Observability Analysis

A minimum number of real-time measurements are needed to calculate and estimate the system states. An analytical way to determine if the available measurement data set are enough to estimate the states completely is known as observability analysis [32]. Observability analysis can be conducted using either fully-coupled or decoupled measurement equations. Use of fully-coupled model has its drawbacks, the non-uniqueness of the solution being one example [27]. Network observability analysis can also be achieved using topological or numerical methods. Topological methods use decoupled measurement model and graph theory. Numerical approaches may use fully-coupled or decoupled models. These methods are formulated using either branch or nodal variables and are explained in [27]. The general numerical method which is developed based on branch variables were discussed in [33].

A complete theory of network observability was presented in [34]. Starting from a fundamental notion of the observability of a network, a number of basic facts relating to network observability, unobservable states, unobservable branches, observable islands, relevancy of measurements, etc. were discussed. On top of that, [35] presented a comprehensive observability or/and measurement placement algorithm based on [34]'s theory of network observability. This algorithm is able to deal with the diverse measurement classes: actual, virtual, pseudo, and quasi- available to state estimators in electric utility energy control centers. The algorithm was an extension of earlier SE functions and could handle large power networks.

In the meantime, a new observability algorithm was developed by [36] to determine the phase-angle observability of networks containing line-current-magnitude measurements. The main contribution of this method was its ability to process currents and thus facilitate their use to extend observable islands for a given system. It was shown that the proposed algorithm could be used to test observability of networks which would otherwise be unobservable by prior methods based on the rank of the measurement Jacobian. While the proposed procedure was developed only for phase-angle observability, it could be extended to cases where the redundant line currents would also be used to observe the voltage magnitudes. Determining observability of power networks based on artificial neural network technique was also proposed in [37].

2.1.3 Bad Data Analysis

One of the essential functions of a state estimator is to detect bad measurements and to identify and eliminate them accordingly [38]. Bad data analysis could be performed during the estimation process or post-estimation. When using the Weighted Least Squares (WLS) estimation algorithm for SE, detection and identification of bad data is done after the estimation process by processing the measurement residuals. The analysis is essentially based on the properties of the residuals, including their expected probability distribution.

Chi-squares test for bad data detection was presented in [27],[39]. It uses the properties of the chi-squares probability density function to compare with the objective function of WLS. Chi-squares was able to detect bad data but does not identify locations.

Alternatively, Largest Normalized Residual Test (LNRT) was able to detect as well as identify the locations of occurrences [27] [38] and[40]. LNRT was developed based on the statistical characteristics of the measurement residuals. Detection and identification could also be accomplished by further processing of the residuals as in the Hypothesis Testing Identification (HTI) methods [27, 38, 41]. Although both methods used the residual sensitivity matrix to represent the sensitivity of the measurement residuals to the measurement errors, HTI was more complex and computationally costly due to the further processing of the residuals. Hence, LNRT was used to detect and identify bad data in this thesis.

However, LNRT was observed to exhibit some limitations as noted in [27]. The primary limitation was the inability to track bad data if it occurred at critical locations. To resolve this issue, utilizations of PMU measurements were proposed in recent literature and are summarized in the upcoming section.

2.2 Measurement and Communication Devices

The field of monitoring and control of power systems are conventionally operated using SCADA systems [7]. The continuous growth of the power networks and increased integration of Variable Energy Resources (VER) triggered challenges to traditional SCADA systems. This led to the introduction of new technologies such as PMUs [42]. Today, PMU technology serves as the next step in improving the quality of the estimate of the system states. They provide operators better information to maintain a high level of system reliability. As a result, PMUs have become a research focus for finding on better ways to integrate them into the state estimation problem as well as other power system applications [43-46]. While incorporating PMU measurements are still noticeably more expensive than traditional RTU approach, PMU deployment to build a hybrid setup with traditional SCADA systems may give additional operating benefits to SE. This is an emerging field of SE.

2.2.1 Summary of PMU Technology

A PMU or synchrophasor is a device that measures the electrical phasor in an electric grid using a common time source for synchronization. It provides real time information in a time-synchronized way, and is a solution to improve the monitoring, protection and control of future electric grid. In typical applications, PMUs are sampled from widely dispersed locations in the power network and synchronized from the common time source based on a global positioning system (GPS) [46]. It is possible to achieve synchronization accuracies of 1 μs or better. As one micro-second corresponds to 0.021^{o} for a 60 Hz signal, such accuracies are perfect for measuring power frequency, voltages and currents [46]. A Block diagram of PMUs in power systems is shown in Fig.2.2.

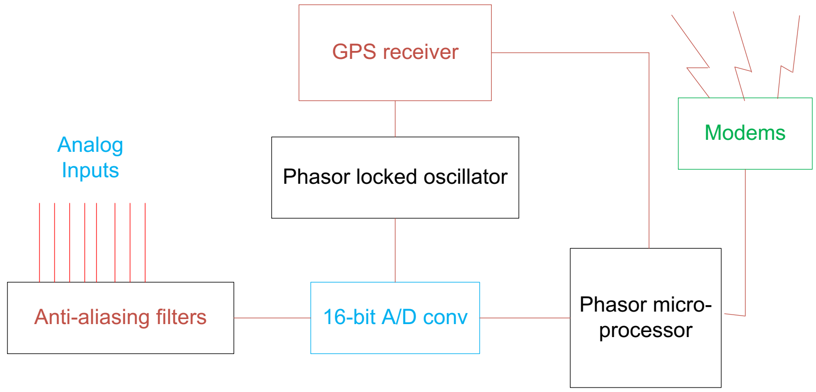

Fig. 2.2 Block diagram of a PMU

2.2.2 Integration of PMU measurements into State Estimation

Conventional state estimations use measurements provided by SCADA systems that consist of bus voltage magnitudes, power flows and injections. These measurements are then related to state variables through measurement functions and the measurement noise. Subsequently, estimation algorithm is run to obtain the estimated state variables of the power system, which are the magnitude and phase angle of voltages at each bus. The most widely commercially used state estimation algorithm, which is nonlinear and iterative, is weighted least squares (WLS) [9].

It was a prevalent idea in most of conventional SEs that the precise and simultaneous collection of measurements across the grid was something that could never be accomplished. The assumption that held conventional SE techniques together was the power system's quasi-static nature; i.e. changing steadily but very slowly, in which operators could afford to have significant scan times. Although some estimators today have a scan time of only a few seconds, this could still be an eternity for several applications in the fields of protection and control [47]. To overcome these issues, integration of PMU measurements into SE is explored in recent years.

Although it is evident that phasor based measurement system is a preferable technique to traditional state estimator techniques, it is recognized that in many cases one cannot provide as sufficient PMU devices capable of achieving this goal. One of the major obstacles that hinder utilities from sufficient deployment of these devices is the prices associated with them [48].

In response to the economic limitations, intensive researches are undergoing to utilize the emerging technologies in a best and optimized manner that could enhance the existing state estimation platforms. As a result, it has been shown that the addition of PMU measurements on top of the traditional ones could substantially increase the quality of the state estimates [49].

A straight forward application of state estimation, used by most state estimators, treats PMU measurements to be supplements to traditional SCADA measurements. The resulting estimator once again follows a nonlinear, iterative solution scheme that needs significant modifications to the existing software to include PMU measurements. But, in [28] an alternative method for including phasor measurements in state estimators was proposed. This scheme preserves the original Energy Management Systems (EMS) software, and includes PMU measurements as a post-processing step. This approach takes the estimated states from the traditional SE and combine them with PMU measurements to conduct a second stage linear SE. Such approach would not require changes to be made to the existing software every time when new PMUs are installed into the network. Hence, making it more economical for utilities to adopt in reasonable matters.

PMUs also play an important role in handling some deficiencies in the traditional measurement set. For example, in improving network observability [32, 35, 37, 50-56], aiding bad data processing [40, 51, 57-61], and determining the network topology.

It should be emphasized that this thesis focuses on the aspects of inclusion of PMUs on state estimation as a post-processing step. The motivation was to enhance the bad data detection capability while improving the accuracy of the state estimates.

2.3 Summary

This chapter discussed the literature review on the developments and methodologies of the overall field of state estimation. The structure of state estimator package found in the EMS which consists of a topology processor, observability analysis, state estimation and bad data analysis was briefly discussed.

The main objective of this thesis is improving the bad data detection capability and hence different techniques on the literature were reviewed. The most widely used detection test is based on the largest normalized residual test. However, it has limitations with setting detection threshold and when it comes to detecting certain type of measurements known as critical measurements. Therefore, this thesis addresses these issues in the coming chapters. The next chapter discusses the mathematical formulation of the estimators used in this thesis.

CHAPTER 3

State Estimation Problem Formulation

Power system state estimation is the process of determining the states of the power systems; which are the voltage magnitudes and voltage angles of each node. It is a mathematical calculation of the states based on measurements collected across the power network. While doing so, it assumed that the system topology is known.

Another important application of state estimators is their ability to identify gross errors in measurement devices provided that there are enough redundant measurements. Moreover, the failure and/or the loss of a device or devices can also be detected. Topology of a network changes when a line is lost due to overloading or equipment failure [62]. In such a case, the security of the system might be in danger since some other lines might get overloaded as well. State estimation results can therefore give early warnings of such cases.

This chapter discusses background of power systems and the basic mathematical modeling of various electrical components and followed by the formulation of the system admittance matrix. The model is then used in the formulation of state estimation algorithms and incorporation of phasor measurement units (PMUs) to improve estimation quality and enhance bad data detection capability.

3.1 Formulation of the System Model

Several factors affect the state of the power system. They include system parameters like resistance, reactance and shunt susceptance of transmission lines. Measurements like real and reactive power injections, active and reactive power flows, measured voltages and network topology (assumed to be known) are also among those factors [27].

Measurements are sent periodically to control centers via SCADA system. But prior to implementation, the transmission line parameters and physical system model are carefully constructed offline. This section discusses the construction of detailed system model and mathematical representation of each component and build system matrices to be used in the state estimation formulations.

3.1.1 Transmission line Model

Transmission lines in power systems are three phase. A fully transposed transmission line is assumed with all the series and shunt devices being symmetrical in all the three phases. Generations and loads at each phase are also assumed balanced [27]. Therefore, single phase analysis is used to simplify the transmission line model, which is represented by a two-port pi model [63]. The equivalent circuit of the transmission line is shown in Fig. 3.1 connecting bus k to m.

Using Kirchhoff's law current injection in bus k and bus m can be written as

$$\begin{bmatrix} I_k \\ I_m \end{bmatrix} = \begin{bmatrix} y + jB & -y \\ -y & y + jB \end{bmatrix} \begin{bmatrix} V_k \\ V_m \end{bmatrix} \tag{3.1}$$

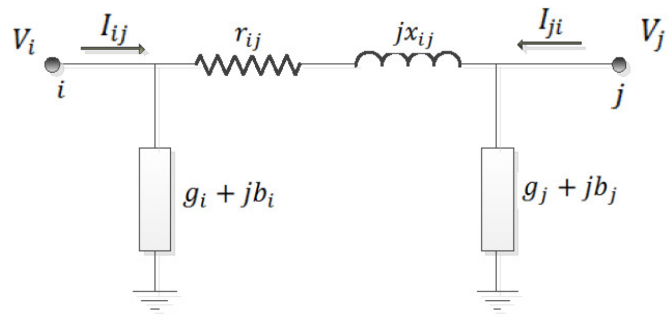

Fig. 3.1: Two-port π model of a transmission line

Where, $$y = \frac{1}{R + jX}$$

3.1.2 Shunt Reactor and Capacitor Models

Shunt reactors or capacitors are represented by their per phase susceptance value. They are mainly used for voltage and/or reactive power support. The type of the shunt element is determined by the value of the susceptance at the corresponding Bus. It is positive for a capacitor and negative for a reactor [27].

3.1.3 Tap Changing Transformer Model

Tap changing transformers are used to step up or step down voltage by a scalar quantity '*a*' known as the tap ratio without affecting the voltage phase angle. It is modeled as a series impedance in series with an ideal transformer in between Bus k and Bus m as shown in Fig. 3.2.

3.1.4 Generators and Loads Models

Generators and loads are represented as power injections into their corresponding Buses and therefore have no effect. Generators are treated as positive injection and loads as negative injection.

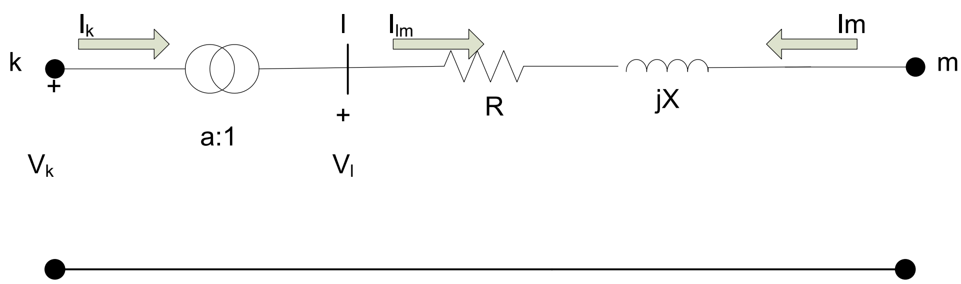

Fig. 3.2: Equivalent circuit of a tap-changing transformer

The following equations illustrate the relationship among the parameters of the transformer in figure 3.3.

$$v_1 = \frac{1}{a} v_k \tag{3.2}$$

$$i_{lm} = a i_k \tag{3.3}$$

$$i_{lm} = y(v_1 - v_m) \tag{3.4}$$

Substituting v_l and i_{lm} and re-arranging equations (3.2) - (3.4), we get

$$a i_k = y(\frac{1}{a} v_k - v_m) \tag{3.5}$$

$$i_k = \frac{y}{a^2} v_k - \frac{y}{a} v_m \tag{3.6}$$

And

$$i_m = -i_{lm} = y(v_m - v_l) \tag{3.7}$$

Then substituting v_l

$$i_m = y v_m - \frac{y}{a} v_k \tag{3.8}$$

Finally putting in matrix form, we get

$$\begin{bmatrix} I_k \\ I_m \end{bmatrix} = \begin{bmatrix} y/a^2 & -y/a \\ -y/a & y \end{bmatrix} \begin{bmatrix} V_k \\ V_m \end{bmatrix} \tag{3.9}$$

Therefore using the above equations a simplified model as shown in Fig. 3.3 can be formulated.

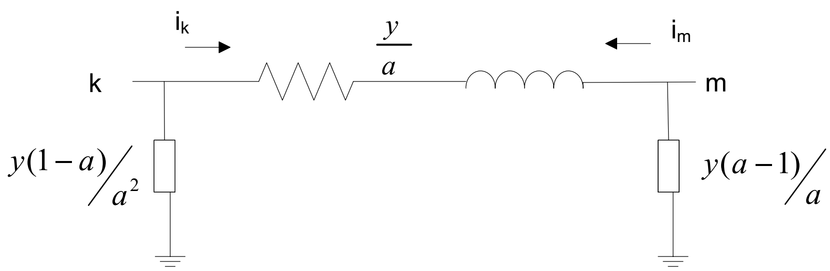

Fig. 3.3 Equivalent circuit for an in-phase transformer tap changer

Similarly when it is a phase shifting transformer the equations are changed slightly since unlike a tap-changer a phase-shifter has a complex tap ratio, represented by *a* below. Since the main purpose of a phase shifter is controlling the flow of power and prevent congestion, it creates a phase difference between the primary and secondary voltages. The changes in the equations are as shown below.

$$v_l = \frac{1}{a} v_k \tag{3.10}$$

$$i_{lm} = a * i_k \tag{3.11}$$

Substituting into the matrix, gives the following

$$\begin{bmatrix} I_k \\ I_m \end{bmatrix} = \begin{bmatrix} y/|a|^2 & -y/a* \\ -y/a & y \end{bmatrix} \begin{bmatrix} V_k \\ V_m \end{bmatrix} \tag{3.12}$$

3.2 Y-Bus Admittance Matrix formulation

Referring to the modeled network parameters, we can now represent the entire power system as an admittance matrix commonly known as the Y-Bus matrix. A general Y-Bus representation of a system with N buses is shown in (3.13)

$$\begin{bmatrix} i_1 \\ i_2 \\ \vdots \\ i_N \end{bmatrix} = \begin{bmatrix} Y_{11} & Y_{12} & \cdots & Y_{1N} \\ Y_{21} & Y_{22} & \cdots & Y_{2N} \\ \vdots & \vdots & \ddots & \vdots \\ Y_{N1} & Y_{N2} & \cdots & Y_{NN} \end{bmatrix} \begin{bmatrix} V_1 \\ V_2 \\ \vdots \\ V_N \end{bmatrix} = \text{Y x V} \tag{3.13}$$

The Y-Bus is formulated using an admittance matrix. It is very difficult to populate the matrix with impedance values while it is easier to populate it with system admittances even by inspection. Kirchhoff's current law is applied when populating the admittance matrices. The following two rules summarize the procedure to populate the Y-Bus by inspection.

- The iith element of the Y-Bus denotes the sum of all admittances directly connected to Bus i. This includes shunt susceptances and shunt capacitors and reactors of the lines connected Bus i.
- ijth element of the Y-Bus denotes the negative admittance of the line between Bus i and Bus j.

After populating the Y-Bus matrix, we include the transformer parameters into the Y-Bus by modifying the Y-Bus corresponding to the locations of installed transformer. Consider a transformer between Bus k and Bus m, then four entries of the Y-Bus elements should be updated as:

$$Y_{kk}^{new} = Y_{kk} + {y}/{|a|^2} \tag{3.14}$$

$$Y_{km}^{new} = Y_{km} - {y}/{a^*} \tag{3.15}$$

$$Y_{mk}^{new} = Y_{mk} - {y}/{a} \tag{3.16}$$

$$Y_{mm}^{new} = Y_{mm} + y \tag{3.17}$$

3.3 Maximum Likelihood Estimation

The main objective of state estimation is to estimate the most likely states of a power system based on a set of measurements. One way to accomplish this is to use maximum likelihood estimation (MLE), a method widely used in the field of statistics. MLE is the mathematical theory empowering state estimation techniques. It starts from creating the likelihood function of the measurement vector.

Assuming the measurements are independent of each other, the likelihood function is simply the product of each of the probability density functions of each measurement. MLE aims to estimate the unknown parameters of each of the measurements' probability density functions through an optimization [27]. It is commonly assumed that the probability density function (pdf) for measurement errors is the standard normal probability density function.

$$f(z) = \frac{1}{\sqrt{2\pi\sigma}} e^{-\frac{1}{2}(\frac{z-\mu}{\sigma})^2} \tag{3.18}$$

where z is the random variable of the pdf, μ is the mean, and σ is the standard deviation. This function would yield the probability of a measurement being a particular value, z. Therefore, the probability of measuring a particular set of m measurements each with the same probability density function is the product of each of the measurements probability density functions, or the likelihood function for that particular measurement vector [27].

$$f_m(z) = \prod_{i=1}^{m} f(z_i) \tag{3.19}$$

Where z_i is the ith measurement and

$$z = \begin{bmatrix} z_1 \\ z_2 \\ \vdots \\ z_m \end{bmatrix} \tag{3.20}$$

f_m is called the likelihood function for z which is the measure of the probability of observing the specific set of measurements in vector z. Therefore, MLE's objective is to maximize this function to determine the unknown parameters of the pdf of each measurement. This is done by maximizing the logarithm of the function, $f_m(z)$,

$$\log f_m(z) = \sum_{i=1}^{m} \log f(z_i) = -\frac{1}{2}\sum_{i=1}^{m}\left(\frac{z_i - \mu_i}{\sigma_i}\right)^2 - \frac{m}{2}\log 2\pi - \sum_{i=1}^{m}\log\sigma_i \quad (3.21)$$

or minimizing the weighted sum of the squares of the residuals [27]

$$\text{Minimize } \sum_{i=1}^{m}\left(\frac{z_i - \mu_i}{\sigma_i}\right)^2 \qquad (3.22)$$

This can therefore be written as:

$$\textit{Minimize } \sum_{i=1}^{m} W_{ii} r_i^2 \qquad (3.23)$$

$$\textit{Subject to } z_i = h_i(x) + r_i$$

Where W is the weighting factor given as $W_{ii} = \sigma_i^{-2}$. The solution to this problem gives us the weighted least squares estimator, which would be explained in the following subsection.

3.4 Weighted Least Squares Based Estimator

State estimators use information from measurements dispersed across the power grid to determine the most likely state variables. Measurement devices may have different accuracies and therefore are treated differently. Measurement error covariance is used to weight the accuracy of the measurements during this process, hence the name 'weighted least squares'. The network system model and the set of measurements make up the equality constraints of the WLS optimization and make the problem specific to power systems.

Consider a measurement vector z with m number of measurements, which contain unknown measurement errors e associated with the limited accuracy of measurement devices. The errors are assumed to be independent to each other, and are normally distributed with an expected value of zero. Therefore, the equation relating measurements to system states x, containing n state variables, can be written as:

$$z = \begin{bmatrix} z_1 \\ z_2 \\ \vdots \\ z_m \end{bmatrix} = \begin{bmatrix} h_1(x_1, x_2, \cdots, x_n) \\ h_2(x_1, x_2, \cdots, x_n) \\ \vdots \\ h_m(x_1, x_2, \cdots, x_n) \end{bmatrix} + \begin{bmatrix} e_1 \\ e_2 \\ \vdots \\ e_m \end{bmatrix} = h(x) + e \tag{3.24}$$

Where h is a nonlinear equation relating the state vector x to measurements z. The states are voltage magnitudes and angles of each node. As discussed in MLE, the solution to the state estimation problem is formulated as an optimization problem, whose objective function is denoted as J . As indicated in (3.25), the least squares errors of measurement residuals are weighted by their respective measurement error covariance specified by R.

$$J(x) = \sum_{i=1}^{m} \frac{(z_i - h_i(x))^2}{R_{ii}} \tag{3.25}$$

Equation (3.25) represents the summation of the squares of the measurement residuals weighted by their respective measurement error covariance and can be rewritten as:

$$J(x) = \frac{1}{2}[z - h(x)]^T R^{-1} [z - h(x)] \tag{3.26}$$

Where R is the diagonal matrix representing the measurement error covariance matrix, which is the weighting factor:

$$R = \begin{bmatrix} \sigma_1^2 & & & \\ & \sigma_2^2 & & \\ & & \ddots & \\ & & & \sigma_m^2 \end{bmatrix}$$

Where σ_i^2 is the variance of each of the measurement errors which are assumed to be normally distributed and denoted as: $e_i \sim N(0,R)$ for all i.

Now, since our objective is minimization of the objective function J, we can find the derivative of J and set it to zero to find the minimum. Consider the derivative of J denoted by g(x) as:

$$g(x) = \frac{\partial J(x)}{\partial x} = -H^T R^{-1}[z - h(x)] \tag{3.27}$$

Where *H* is the measurement Jacobian matrix and is given by:

$$H(x) = \frac{\partial h(x)}{\partial x} \tag{3.28}$$

Expanding the non-linear function g into its Taylor series around the state vector x^k gives:

$$g(x) = g(x^k) + G(x^k)(x - x^k) + \ldots = 0 \tag{3.29}$$

$$\text{In which } G(x^k) = \frac{\partial g(x)}{\partial x} = H^T R^{-1} H \tag{3.30}$$

Then if we ignore the higher order terms of the series expansion, the differential of J gives a final iterative solution known as Gauss-Newton method given in (3.31)

$$x^{k+1} = x^k + G(x^k)^{-1} H^T R^{-1}(z^k - h(x^k)) \tag{3.31}$$

Or substituting Δx

$$x^{k+1} = x^k + \Delta x \tag{3.32}$$

- The measurement function *h* is constructed using the known system model which consist of branch parameters, network topology, and measurement locations and type.
- Then measurement Jacobian *H* is found by differentiating *h* with respect to state vector *x.*
- R is the error covariance matrix holding information of the metering accuracy and should be formulated prior to computation.
- k is the iteration index
- *G* is called the gain matrix and is sparse, positive definite and symmetric provided that the system is fully observable. *G* is typically not inverted (the inverse will in general be a full matrix, whereas *G* itself is quite sparse).

Flat start, i.e. setting the voltage magnitudes to one and phase angles to zero, is assumed for initializing the iteration and measurement function and jacobian are calculated accordingly. Iterations are carried out till a certain predefined threshold value is reached.

3.5 Iterated Extended Kalman Filter (IEKF) based Estimator

This section illustrates the formulation of the IEKF based estimator. Here the actual dynamics of the static states is formulated and hence a model for the transition of states needs to be generated. This model is then used to formulate the Kalman filter. Therefore a pseudo-dynamic model was generated through the linearization of the power flow equations as in [30] and shown in (3.33).

$$\tilde{V}_i \sum_j (\tilde{V}_j Y_{ij})^* = P_i + jQ_i \tag{3.33}$$

Where $\tilde{V}_i$ is the complex voltage phasor at bus i, Y_{ij} is the $(i,j)^{th}$ elements of the Ybus matrix and P_i and Q_i are the active and reactive power injections at bus i.

Defining the active and reactive injections at each bus as a vector *u:*

$$u = [P_1 \cdots P_N Q_1 \cdots Q_N]^T \tag{3.34}$$

and then rewriting (3.33) in terms of power injections u and state variables x, we can get (3.35).

$$g(x,u) = [g_p(x,u) \quad g_Q(x,u)]^T \tag{3.35}$$

Where,

$$\begin{aligned} g_P &= P_i - V_i \sum_{j=1}^{N} V_j [G_{ij} \cos\theta_{ij} + B_{ij} \sin\theta_{ij} = 0 \\ g_Q &= Q_i - V_i \sum_{j=1}^{N} V_j [G_{ij} \sin\theta_{ij} - B_{ij} \cos\theta_{ij} = 0 \end{aligned} \tag{3.36}$$

The piecewise linearization of (3.36) would then result to (3.37),

$$\frac{\partial g(x,u)}{\partial x} \Delta x + \frac{\partial g(x,u)}{\partial u} \Delta u + e \;\; = 0 \tag{3.37}$$

The partial derivatives can be further illustrated as:

$$\frac{\partial f(x,u)}{\partial x} = \begin{bmatrix} \frac{\partial f_p}{\partial \delta} & \frac{\partial f_p}{\partial V} \\ \frac{\partial f_Q}{\partial \delta} & \frac{\partial f_Q}{\partial V} \end{bmatrix} = J \tag{3.38}$$

Which is a Jacobian of the power flow equations and

$$\frac{\partial f(x,u)}{\partial u} = \begin{bmatrix} \frac{\partial f_p}{\partial P} & \frac{\partial f_p}{\partial Q} \\ \frac{\partial f_Q}{\partial P} & \frac{\partial f_Q}{\partial Q} \end{bmatrix} = \begin{bmatrix} I & 0 \\ 0 & I \end{bmatrix} = I \tag{3.39}$$

An identity matrix. Substituting equations (3.38) and (3.39) in (3.37) and solving for the change in state variables Δx, and rearranging we get:

$$x_k = x_{k-1} + J_k^{-1}[u_k - u_{k-1}] + J_k^{-1}e \tag{3.40}$$

Where $J_k^{-1}e$ corresponds to system process noise.

Equation (3.40) is a pseudo-dynamic model of the system network. This equation is then used in the prediction step of the Kalman filter based estimator. In the prediction step, state variables are estimated using the previous states and corrected in the correction step when the measurement set is obtained [31]. This two-step estimation is shown as:

$$\text{Prediction}\begin{cases} x_k = x_{k-1} + J^{-1}[u_k - u_{k-1}] \\ P_{k,0} = P_{k-1} + Q \end{cases} \tag{3.41}$$

$$\text{Correction}\begin{cases} K_{k,i} = P_{k,i-1}H'_{k,i-1}(H_{k,i-1}P_{k,i-1}H'_{k,i-1} + R)^{-1} \\ x_{k,i} = x_{k,i-1} + K_{k,i}[z_k - h_{k,i-1}] \\ P_{k,i} = (I - K_{k,i}H_{k,i-1})P_{k,i-1} \end{cases} \tag{3.42}$$

Where:

- P_k is the state error covariance matrix at time step k
- Q is process covariance matrix, approximations introduced to linearization of the process noise caused due to linearization errors.
- $K_{k,i}$ is the Kalman gain at time step k and iteration i.
- R is the measurement covariance matrix
- H is the Jacobian matrix of the measurement function h
- z is measurement vector and
- i is the iteration index in the correction step

3.6 Summary

This chapter discussed the mathematical formulations of the state estimators used in this thesis. Modelling of the system network transmission lines, shunt reactors and capacitors, generators and loads leading to the formation of the admittance matrix was discussed in detail. The model was used for basic formulations of the WLS and IEKF estimation algorithms. The next chapter discusses bad data analysis and techniques proposed to improve detection and identification.

CHAPTER 4

Bad Data Detection

Measurements collected from across the network are used as input to state estimators to determine the best likely states of the system. This provides important information for monitoring and control functions whose objective is delivering secured and reliable power to customers. It is also important to suspect the reliability of the measurements which otherwise could affect estimation results. Therefore measurement error detection, identification and elimination should be an integral part of state estimators [27, 64]. There are four types of errors which state estimation algorithms should be able to handle [27].

- Measurements errors: errors that exist due to limited accuracy of measurement devices
- Topology errors: errors caused from an incorrect topological information
- Parameter errors: errors caused from uncertainties in modelling parameter like line admittances
- Bad data: large measurement errors caused due to malfunctioning, aging, bias or misconnection of measurement devices.

Since the scope of this thesis is dealing with large measurement errors, hence this chapter discusses bad data caused by the fourth category (bad data) of error types. Treatment of bad data depends on the method of state estimation used in the implementation. With the commonly used WLS method, detection and identification of bad data are done after the estimation solution by analyzing the measurement residuals. This chapter discusses bad data detection techniques on WLS and incorporating PMUs to improve the detection capability.

Power systems have different measurement types spread across the grid. They have different properties and estimation results depend on their values and on their locations as well. There should be enough distribution of measurements to ensure network observability.

4.1 Largest Normalized Residual Test (LNRT)

Consider the linearized measurement equation, which is used at each iteration during the numerical solution of the WLS estimation problem:

$$\Delta z = H\Delta x + e \tag{4.1}$$

Applying the optimization criterion, the following expression can be derived for the optimal state update:

$$\begin{aligned}\Delta\hat{x} &= (H^T R^{-1} H)^{-1} H^T R^{-1} \Delta z \\ &= G^{-1} H^T R^{-1} \Delta z\end{aligned} \tag{4.2}$$

The estimated measurement calculated based on the estimated states is given by:

$$\begin{aligned}\Delta\hat{z} &= H\Delta\hat{x} = HG^{-1} H^T R^{-1} \Delta z \\ &= K\Delta z\end{aligned} \tag{4.3}$$

Where $K = HG^{-1}H^T R^{-1}$ is commonly known as the hat matrix since it gives z a hat and has the following property.

$$K \cdot H = H \tag{4.4}$$

Measurement residuals can then be expressed as:

$$r = \Delta z - \hat{z} \tag{4.5}$$

$$
\begin{aligned}
&= (I - K)\Delta z \\
&= (I - K)(H\Delta x + e) \\
&= (I - K)e \\
&= Se
\end{aligned} \tag{4.6}
$$

Where $S = I\text{-}K$, is called the sensitivity matrix and has the following property $S \cdot R \cdot S^T = S \cdot R$. It represents sensitivity of measurement residuals to measurement errors.

As discussed in previous sections, the measurement errors are assumed to have normal distribution and hence the statistic properties of the residual can then be derived as:

- Mean: $E(r) = E(S \cdot e) = S \cdot E(e) = 0$
- Covariance:

$$
\begin{aligned}
&Cov(r) = \Omega = E[rr^T] \\
&= S \cdot E[ee^T] \cdot S^T \\
&= SRS = SR \\
&= R - H \cdot G^{-1} \cdot H^T
\end{aligned} \tag{4.7}
$$

Where Ω is the covariance matrix of the residual.

Hence, measurement residuals are normally distributed with zero mean and Ω covariance. Ω is real and symmetric [2].

The normalized residual for i$^{\text{th}}$ measurement can be calculated as:

$$
r_i^N = \frac{|r_i|}{\sqrt{\Omega_{ii}}} = \frac{|r_i|}{\sqrt{R_{ii} \cdot S_{ii}}}, i = 1, \ldots, m \tag{4.8}
$$

Where vector r^N has a standard normal distribution i.e. $N \sim (0,1)$.

The measurement residual covariance matrix (Ω) has some properties discussed in [2] one of the properties being determining the nature of measurements. If all elements of a row or a column are zero, then the measurement corresponding to that row or column is a critical measurement [27].

Once residuals are normalized then they are tested for information on measurements for analysis processes such as bad data detection. Provided there is enough redundancy, the elements of the normalized residual r^N are then compared to a predefined threshold and if there exists a value greater than the threshold, then the measurement corresponding to that residual is suspected to contain bad data and should be removed. The following steps are followed to detect and identify bad data using LNRT.

- Solve WLS problem and calculate measurement residuals $r = z - h(\hat{x}))$
- Calculate normalized residuals $r_i^N = \frac{|r_i|}{\sqrt{\Omega_{ii}}} = \frac{|r_i|}{\sqrt{R_{ii} \cdot S_{ii}}}, i = 1,\ldots,m$
- Find the largest value r_k^N in the normalized residual corresponding to k^{th} measurement;
- If $r_k^N > \varepsilon$ then the k^{th} measurement is identified as bad data otherwise, no bad data will be suspected. Here ε is the chosen identification threshold.
- Eliminate k^{th} measurement and repeat state estimation process.

4.2 Bad Data on Critical Measurements

As stated in previous sections bad data coming from critical measurements is undetectable using conventional LNRT. Critical measurements can be identified from the property of the covariance matrix of the residual Ω. If all elements of a row or column of the matrix are zero, then the measurement corresponding to that row or column are critical measurements and cannot be detected.

To improve this detection capability PMUs are strategically placed to add redundancy and remove critical measurements so that they are easily detected when containing gross errors [57, 64, 65]. Once they are no longer critical measurements they can easily be detected by the scheme.

PMU incorporation into an existing state estimation has been shown in several literatures. There are two types of methodologies for including PMUs into existing conventional state estimators namely:

- Mixed PMUs and conventional measurements: in this scheme, a major change takes place in the existing state estimation software to accommodate the additional PMUs in the process, as illustrated in Fig.4.1
- Post-processor: in this scheme PMUs are added as a linear problem after the conventional estimation process has already taken place. Here the existing estimation software remains untouched and instead, its estimated state results are used as inputs to the linear post processing process estimation as illustrated in Fig 4.2. The equivalence of both methodologies is shown in [28]

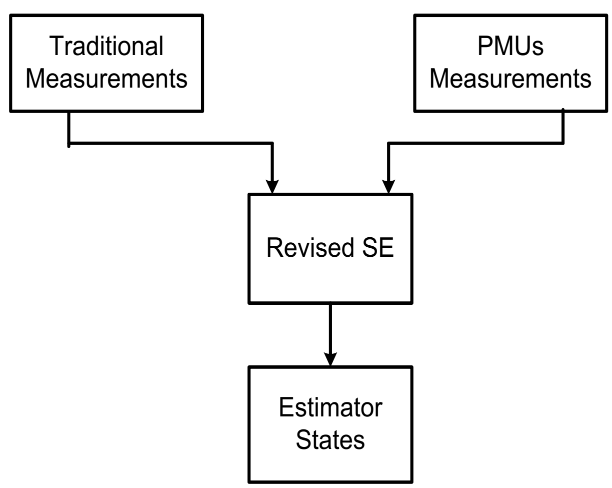

Fig. 4.1 Mixed PMU with traditional measurements

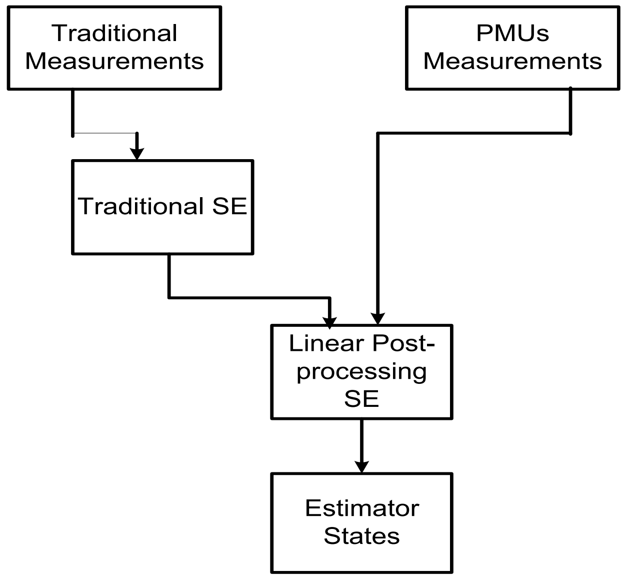

Fig. 4.2 Post-processing step

4.3 Incorporation of PMUs

In this thesis, the post-processing step was implemented by strategically placing the PMUs to enhance the bad data detection capability by eliminating critical measurements while also improving the estimation results. Firstly the PMU measurements must be converted from polar to rectangular coordinates and the associated covariance matrix must be transformed accordingly [28].

$$\mathrm{cov}(x)_{rect} = R'\,\mathrm{cov}(x)R'^{T} \tag{4.9}$$

Where R is a rotation matrix used to transform the covariance matrix to correspond to rectangular coordinates instead of polar coordinates. Then, the calculated system state and the phasor measurement vector could be vertically concatenated and related to the system state by a linear equation.

Then, the estimated system states from the conventional estimator serve as measurement inputs for the linear post-processor and are vertically concatenated with phasor measurements as:

$$z_{new} = \begin{bmatrix} x_{conv} \\ z_{pmu} \end{bmatrix} = \begin{bmatrix} V_r \\ V_i \\ V_{r\_pmu} \\ V_{i\_pmu} \\ I_r \\ I_i \end{bmatrix} \tag{4.10}$$

Where x_{conv} is the state vector obtained from the conventional state estimator represented in rectangular coordinates V_r and V_i as the real and imaginary voltages of each Bus and similarly V_{r_pmu} and V_{i_pmu} are real and imaginary values of voltage measurements from PMUs. I_r and I_i are real and imaginary current values from PMUs. The new measurement vector z_{new} is linearly related to the new state vector x_{new} by forming a H_{new} matrix as shown in (4.11)

$$z_{new} = H_{new} x_{new} = \begin{bmatrix} I & 0 \\ 0 & I \\ I' & 0 \\ 0 & I' \\ C1 & C2 \\ C3 & C4 \end{bmatrix} \begin{bmatrix} V_{r\_pmu} \\ V_{i\_pmu} \end{bmatrix} \tag{4.11}$$

The 'I' in the above equation represents a unit matrix, whereas the 'I'' represents a unit matrix with zeros on the diagonal where no voltage phasors have been measured. In (3.11), it can be observed that the system state is identically related to the partition of the measurement vector which contains the calculated system state and identically related to the voltage phasor measurements in the measurement vector for those Buses that contain PMUs.

The matrices C1 to C4 are composed of line conductance and susceptances for those lines where current phasor measurements are available. For example, consider the current measurement I_{jk} in line 'jk'. Using the line admittance data used in chapter 2,

$$\begin{bmatrix} I_{(jk)r} \\ I_{(jk)i} \end{bmatrix} = \begin{bmatrix} g_{(jk)} & -g_{(jk)} & \{-b_{(jk)} - b_{(j0)}\} & b_{(jk)} \\ \{b_{(jk)} + b_{(j0)}\} & b_{(jk)} & g_{(jk)} & -g_{(jk)} \end{bmatrix} \begin{bmatrix} V_{(j)r} \\ V_{(k)r} \\ V_{(j)i} \\ V_{(k)i} \end{bmatrix} \tag{4.12}$$

The 'C' matrices are similar to the Bus admittance matrix, with only those non-zero entries that correspond to lines where current phasors are measured.

Equation (3.11) is a linear problem whose solution leads to a WLS solution given as:

$$x_{new} = \left[H_{new}{}^{T} R_{new}{}^{-1} H_{new}\right]^{-1} \left[R_{new}{}^{-1} H_{new}\right] \left[z_{new}\right] \tag{4.13}$$

Where R_{new} is the new covariance matrix which includes both the error models for the calculated system state and the phasor measurement vector converted to rectangular form.

$$R_{new} = \begin{bmatrix} R_{conv} & 0 \\ 0 & R'_{pmu} \end{bmatrix} \tag{4.14}$$

It has been presented that strategic placement of PMUs [58] would alter critical measurements on conventional measurements into redundant measurements. PMU measurements can be placed such that they add redundancy to the critical measurements as a result improving bad data detection capability for measurements which otherwise would have gone undetected. Thus, the new covariance matrix important for calculating the new normalized residual, can easily be formulated using the results of the post-processing step [64].

$$\Omega_{new} = R_{conv} - H_{conv} G_{new}^{-1} H_{conv}^{T} \tag{4.15}$$

4.4 Summary

This chapter discussed bad data analysis on WLS based state estimator. LNRT was the technique used for the detection and identification. As discussed in previous chapters, LNRT has limitations with critical measurements. Incorporation of PMUs at selected locations as a post-processing step was proposed and discussed its formulation. The implementations and results are discussed in the next chapter.

CHAPTER 5

Implementation and Evaluations

The main objective of this chapter is to assess the enhanced bad data detection capability. Simulation results and observations to justify the implemented methodologies are presented. In Section 5.1, the system modelling and measurement generation are discussed and is followed by comparisons of WLS and IEKF methods in Section 5.2. Meanwhile, in Section 5.3, a detailed investigation of the detection threshold of LNRT is outlined. Finally, the merits of incorporating PMU measurements on performance of LNRT is demonstrated in Section 5.4.

5.1 Overview of IEEE 14 Bus Test Case

The system parameters for the IEEE 14 Bus test system used for evaluating the algorithms is shown in Figure 5.1. Power flow solutions were obtained using Matpower, and were applied as true values from which the measurement sets were obtained by adding errors. The collected measurements were active and reactive power injections, active and reactive power flows, and voltage magnitude for conventional measurements and voltage and current phasors for PMU measurements.

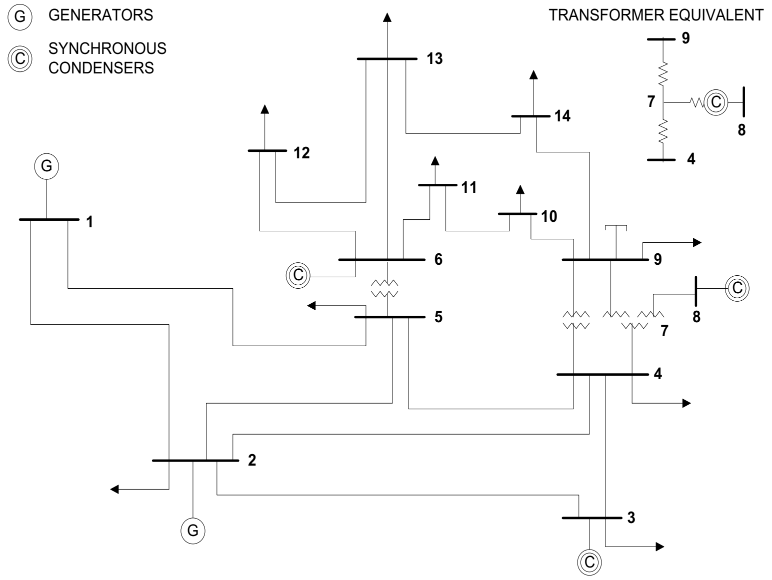

Fig.5.1 IEEE 14 Bus test system

Measurements for conventional SE were collected such that the network becomes observable. An observable system allows the algorithm to converge to a unique solution. PMU measurements consisted of voltage and current phasors. The voltage phasors were directly obtained from the power flow solutions, whereas current measurement between Bus *j* and *k* were calculated as in (5.1) [63]:

$$I_{jk} = \frac{P_{jk} - jQ_{jk}}{V_j^*} \tag{5.1}$$

Errors based on a normal distribution were then added to the measurements as shown below:

$$z_i^{meas} = z_i^{true} + z_i^{true}(randn * \sigma_i) \tag{5.2}$$

Where z_i^{meas} is the measured value, z_i^{true} is the true value obtained from the power flow solution, '*randn'* is a Matlab function for generating normally distributed pseudorandom numbers with N(0,1) and σ_i is the standards deviation of the ith measurement. The standard deviations used are

0.01 for voltage magnitude, 0.02 for power flow and injection measurements, and 0.0005 for PMU measurements.

5.2 Comparisons of WLS Against IEKF

The purpose of this study was to better understand the performance of WLS against another mainstream method known as the Iterative Extended Kalman Filter (IEKF). To summarize, IEKF uses past operating states to predict and estimate the current states. This required modelling the transition between the states, which made the algorithm more complex than WLS. In contrast, WLS takes only a snapshot of the current states, and does not include past state estimates into the computation.

To evaluate the recursive nature of IEKF, assessments were carried out over several monitoring steps. In this study, measurements over 20 time steps were generated and used in the evaluations of IEKF and WLS. They were obtained from the system outlined in Section 5.1. The extracted load profile of Bus 4 is shown in Fig. 5.2.

The parameters used in executing IEKF were:

- Value of process noise Q associated with the linearization error was heuristically set to 0.1 for its diagonal entries.
- State error covariance matrix P was initialized to 10 for its diagonal entries
- State vector x was initialized with a flat start condition. The angles were set to zero and magnitudes to 1.

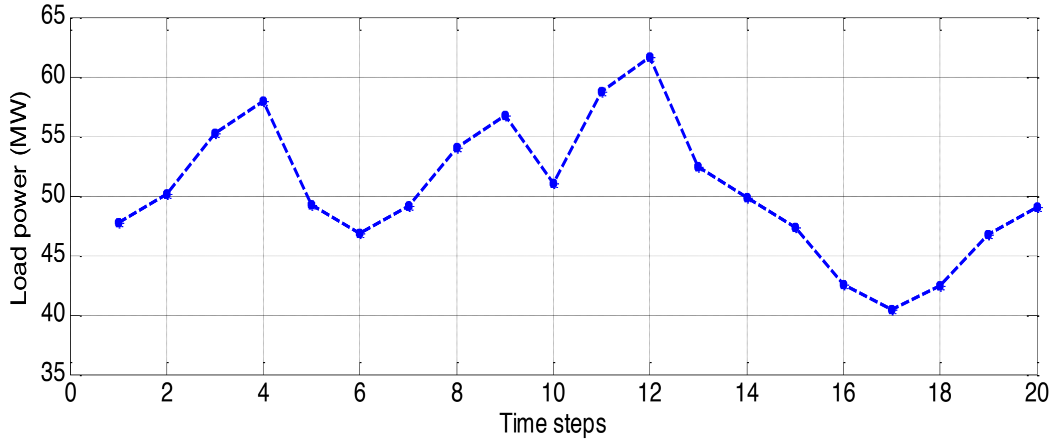

Fig 5.2 Bus 4 load profile

The state vector x for WLS was also initialized with a flat start, but it was reset in every time step. This was due to non-recursive nature of WLS. Fig 5.3 and 5.4 illustrate the procedures followed for executing each algorithm, respectively.

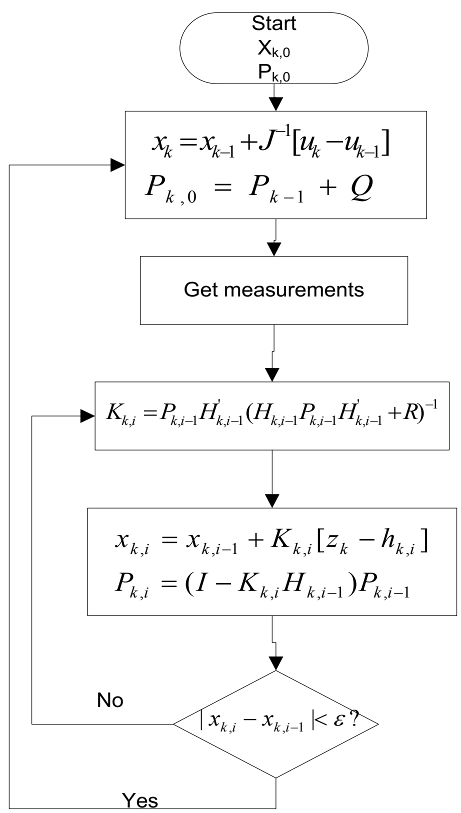

Fig. 5.3 Flow chart implemented IEKF procedures

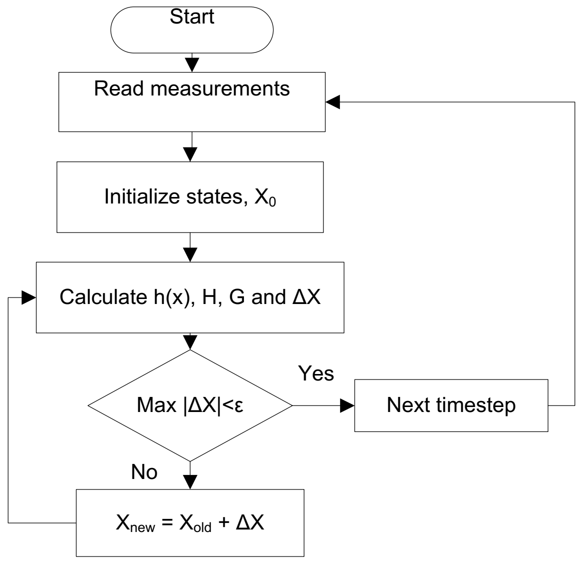

Fig. 5.4: Flow chart of WLS

The performances of IEKF and WLS are illustrated in Fig 5.5 and Fig 5.6. Fig. 5.5 shows the *a posteriori*, i.e. the state estimates of the correction step for Bus 4, while Fig. 5.5 shows the WLS state estimates of Bus 4. Comparing the results, it was evident that WLS was more accurate. One way to examine the accuracy of the estimated states was to determine the voltage mean absolute percentage error (V_MAPE) and angle mean absolute errors (ϴ_MAE) [63]. In this case, the V_MAPE and ϴ_MAE calculated using (5.3) demonstrated that IEKF had 0.0023 and 0.0983 mean errors, respectively. On the other hand, WLS had 0.0011 and 0.0027 for voltage and angle estimations, respectively.

$$\begin{aligned} V\_MAPE &= \frac{1}{m}\sum_{i=1}^{m}\frac{|V_i^{real} - V_i^{est.}|}{V_i^{real}} \\ \theta\_MAPE &= \frac{1}{m}\sum_{i=1}^{m}|\theta_i^{real} - \theta_i^{est.}| \end{aligned} \tag{5.3}$$

The results demonstrated that WLS estimation had more accurate voltage and angle mean errors than IEKF. The difference was significantly larger with angles errors than with magnitudes since the load changes were active power.

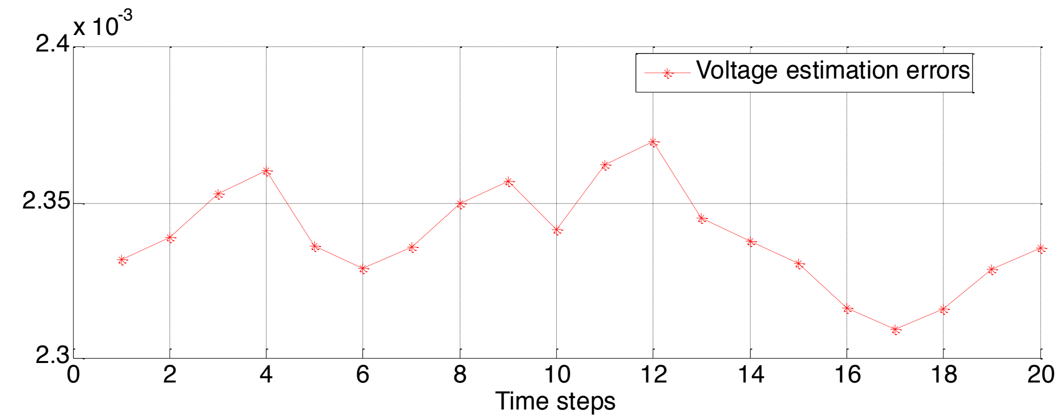

(a)

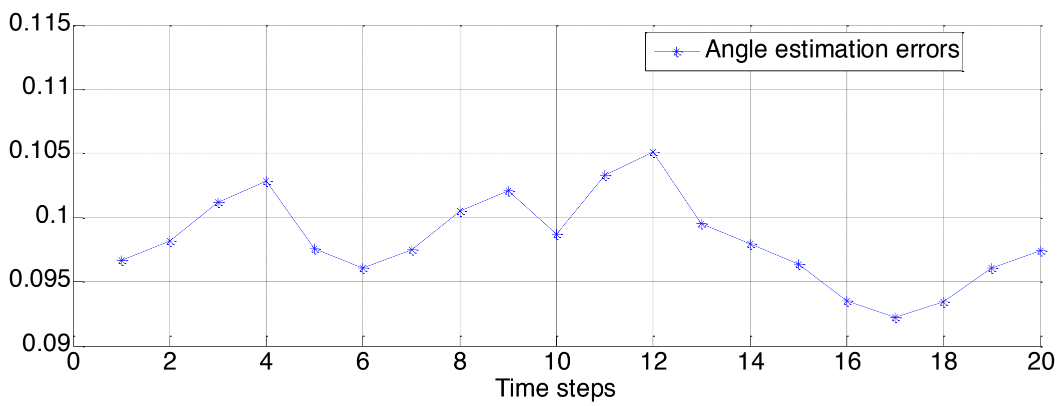

(b)

Fig.5.5 Bus 4 estimations using IEKF

Although IEKF was capable of predicting the next states based on the inputs and relationships of the past states, it was still trailing WLS in the overall state estimation accuracy. Moreover, IEKF contained more sensitive parameters and process noise introduced due to the approximation of the linearization process, and hence made the computation complex and error prone.

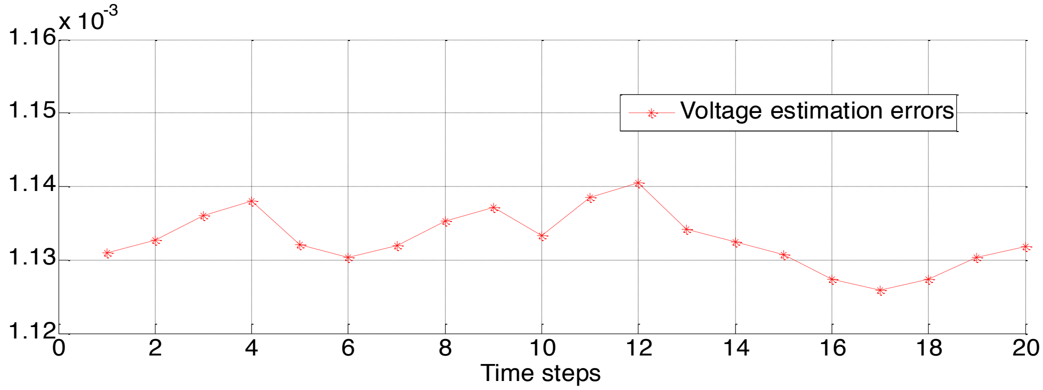

(a)

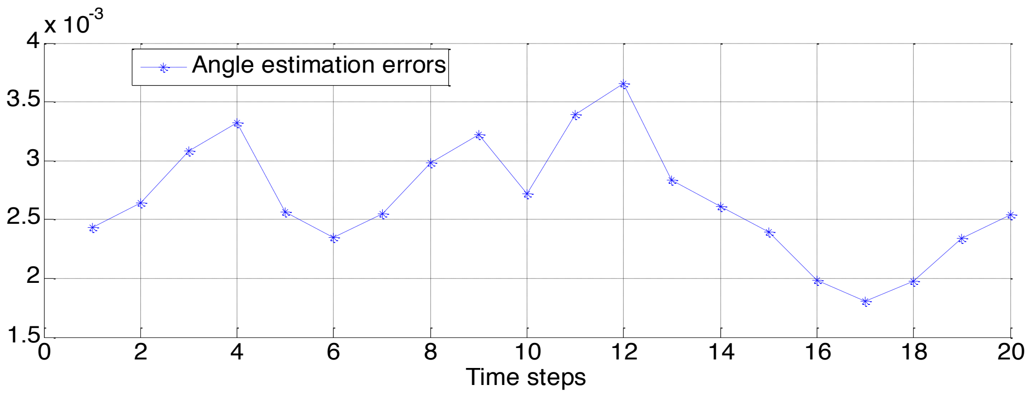

(b)

Fig.5.6 Bus 4 estimations using WLS

5.3 Impact of LNRT Detection Threshold Values

The objective is to study the variations of detection threshold of LNRT against:

- Redundancy ratio and
- Magnitudes of bad data

This was to investigate and verify the variability of detection threshold as compared to fixing it at three, which is the conventionally default value used by state estimators [27]. This was done by changing the redundancy ratio of measurements, and individually injecting bad data of varying magnitudes into arbitrarily chosen sample measurements. Subsequently, the relationship between bad data and detection threshold could be observed. Moreover, the relationship of detection threshold with the redundancy of measurements were also analyzed. Two test cases were built.

Measurements were generated similar to the previous sections, but measurement redundancy was increased here such that there would be no critical measurements. This was because bad data on critical measurements would not be detected using LNRT [27].

Referring to Table 5.1, the first column represents the redundancy ratio and is given as k = m/n. Note that m is number of measurements and n number of states.

Table 5.1: Minimum Errors and corresponding Detection Threshold

Redundancy Ratio	**Measurement type**	**Minimum Error**	**Detection Threshold**
Case 1 k=1.7	P4	0.042	0.748
	Q4	0.005	0.525
	P7-9	0.006	0.535
	Q4-5	0.031	0.542
Case 2 k=2	P4	0.039	0.744
	Q4	0.004	0.515
	P7-9	0.004	0.533
	Q4-5	0.029	0.517

The measurement samples shown for both cases are active (P4) and reactive (Q4) power injections at Bus 4, active power flow from Bus 7 to 9 (P7-9), and reactive power flow from Bus 4 to 5 (Q4-5). Simulations were carried out with incremental injection of errors on each measurement until the error was correctly detected and identified by LNRT. To be detected as bad data, its normalized residual should be the largest of all residuals. This is indicated in Table 5.1. There were two cases with k = 1.7 and k = 2. The middle column labeled ‘Minimum Error’ corresponds to the errors injected such that its detection threshold is reached, i.e. its residual becomes the largest. For example, the active power injection measurement in Bus 4 (P4) was identified as a measurement with flawed data when the error added reached 0.042 p.u., making its corresponding normalized residual to become the largest with a value of 0.748. This was true when k = 1.7, and was lesser (0.744) for k = 2 and was true for all samples. This indicated that with variation of redundancy ratio k, the detection range would increase. Furthermore, the magnitude of error that were identified by LNRT (belong to the largest residual) also decreased (0.042 to 0.039) from Case 1 to Case 2.

Table 5.2: Gross Errors with a Detection Threshold larger than three

Redundancy Ratio	**Measurement Type**	**Gross Error (p.u.)**	**Detection Threshold**
Case 1 k=1.7	P4	0.138	3.017
	Q4	0.111	3.023
	P7-9	0.089	3.007
	Q4-5	0.117	3.017
Case 2 k=2	P4	0.131	3.003
	Q4	0.107	3.014
	P7-9	0.069	3.026
	Q4-5	0.111	3.067

Now, supposed the sensitivity threshold was set to 3. Referring to Table 5.2, additional errors had to be injected to those specific measurements so that LNRT could correctly identify them when the threshold went beyond 3. Here, the 'Gross Error' column referred to the minimum magnitude of error that was injected to a measurement to be picked up by LNRT (meaning threshold > 3). It was observed that the amount of gross error decreases going from Case 1 to Case 2. This demonstrated the value of each measurement residual would vary with k, and contributed to the argument that the sensitivity threshold should not be fixed to a default value. Instead, it should be determined through extensive studies to extend the tracking capability of bad data detection.

Table 5.3: State Estimations without Bad Data

Bus	Voltage (p.u)	Angle (degrees)
1	1.059	0.0
2	1.044	-5.06
3	1.010	-12.88
4	1.017	-10.46
5	1.018	-8.89
6	1.069	-14.40
7	1.058	-13.41
8	1.088	-13.39
9	1.051	-14.98
10	1.047	-15.16
11	1.054	-14.90
12	1.043	-15.09
13	1.028	-14.75
14	1.023	-15.89

For comparative purposes, Table 5.3 serves as a reference showing state estimates obtained without any bad data. Furthermore, Table 5.4 outlines estimation results when gross errors were added to the active power flow measurement P7-9 without defining a fixed sensitivity threshold. The error added to P7-9 in Table 5.4 was 0.042 such that the LNRT identified it as a measurement containing an error without fixing the detection threshold. Lastly, Table 5.5 illustrates the same scenario, except a fixed sensitivity threshold of three was imposed. In Table 5.5, the error injected to P7-9 was 0.138, the minimum amount of error resulting a residual larger than 3. Note results of Table 5.4 and 5.5 are based on Case 1, where k = 1.7. From these results, state estimates were observed to deviate from expected values due to the error margin imposed by assigning a fixed sensitivity threshold of 3. The deviations were mainly captured in angle estimations. In addition, normalized residual of each measurement varied with changes in measurement redundancy. Hence, setting the detection threshold to a fixed value such as three was not effectively consistent in determining the occurrence of a bad data.

Table 5.4: State Estimations with Bad Data injected into P7-9

Bus	**Voltage (p.u)**	**Angle (degrees)**
1	1.059	0.0
2	1.044	-5.06
3	1.010	-12.88
4	1.017	-10.46
5	1.018	-8.89
6	1.069	-14.40
7	1.058	-13.43
8	1.088	-13.39
9	1.051	-15.02
10	1.047	-15.19
11	1.054	-14.90
12	1.043	-15.08
13	1.029	-14.74
14	1.023	-15.92

Table 5.5: State Estimations with Bad Data injected into P7-9 and fixed Detection Threshold

Bus	**Voltage (p.u)**	**Angle (degrees)**
1	1.059	0.0
2	1.044	-5.07
3	1.010	-12.88
4	1.017	-10.49
5	1.018	-8.90
6	1.069	-14.48
7	1.059	-13.52
8	1.088	-13.28
9	1.051	-15.43
10	1.047	-15.52
11	1.055	-15.08
12	1.043	-15.15
13	1.029	-14.82
14	1.023	-16.18

5.4 Evaluation of the Improved LNRT Bad Data Detection using PMUs

As noted in Chapter 2, critical measurements are measurements whose removal from the measurement set would make the system to become unobservable. Thus, bad data contained in these measurements cannot be detected using conventional LNRT. This section investigated the weakness of LNRT when dealing with critical measurements. Subsequently, using PMU measurements to enhance the performance of LNRT was examined. Improvement on the accuracy of state estimation was also investigated. The procedures followed were as follows:

- Identifying critical measurements from the measurement set
- Examining the response of LNRT to bad data at these locations
- Introducing PMUs at selected locations and
- Re-examining LNRT values at critical measurements.

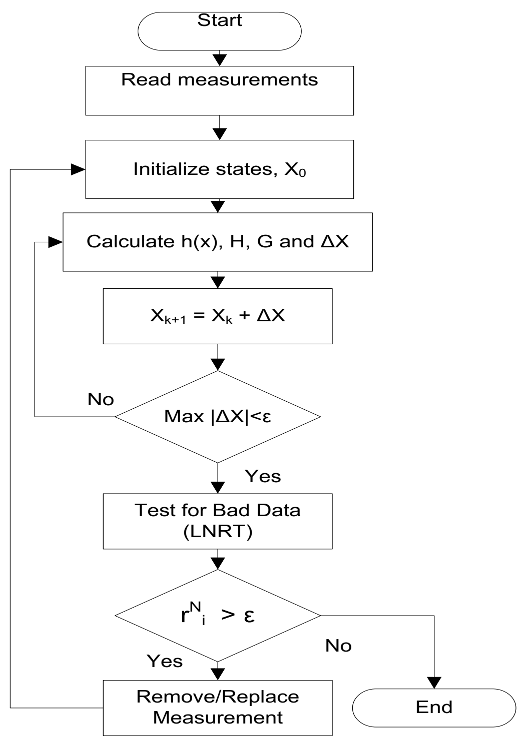

Fig.5.7 Flow chart of LNRT procedure

From the observations made in Section 5.3, the detection threshold used for this study was set to 1 to comfortably detect a range of bad data injections. The basic procedures of bad data detection using LNRT is illustrated in Fig. 5.7. The LNRT test would be carried out after the estimator converged to a unique solution. The performance of the proposed modifications are evaluated as follows.

Firstly, the conventional state estimation results of voltage magnitudes and angles are shown in Table 5.6. Note that no bad data was added, and these results served as comparative references. Their estimation errors (compared with true values) are illustrated in Fig. 5.8. Overall they have a V_MAPE and a Ɵ_MAE of 0.0137 and 0.3082, respectively.

Table 5.6: Voltage magnitude and phase angle estimations

Bus	Voltage (p.u.)	Angle (degrees)
1	1.060	0.00
2	1.045	-5.05
3	1.011	-12.87
4	1.017	-10.44
5	1.019	-8.84
6	1.050	-14.87
7	1.059	-13.42
8	1.086	-17.81
9	1.033	-15.44
10	1.029	-15.64
11	1.036	-15.38
12	1.023	-15.61
13	1.009	-15.27
14	1.004	-16.43

Table 5.7: List of critical measurements

Measurement Type	Bus
Active power injection (Pi)	8,10,11,14
Reactive Power injection (Qi)	8,10,11,14
Active power flow (Pij)	4-7, 6-11
Reactive power flow (Qij)	4-7, 6-11

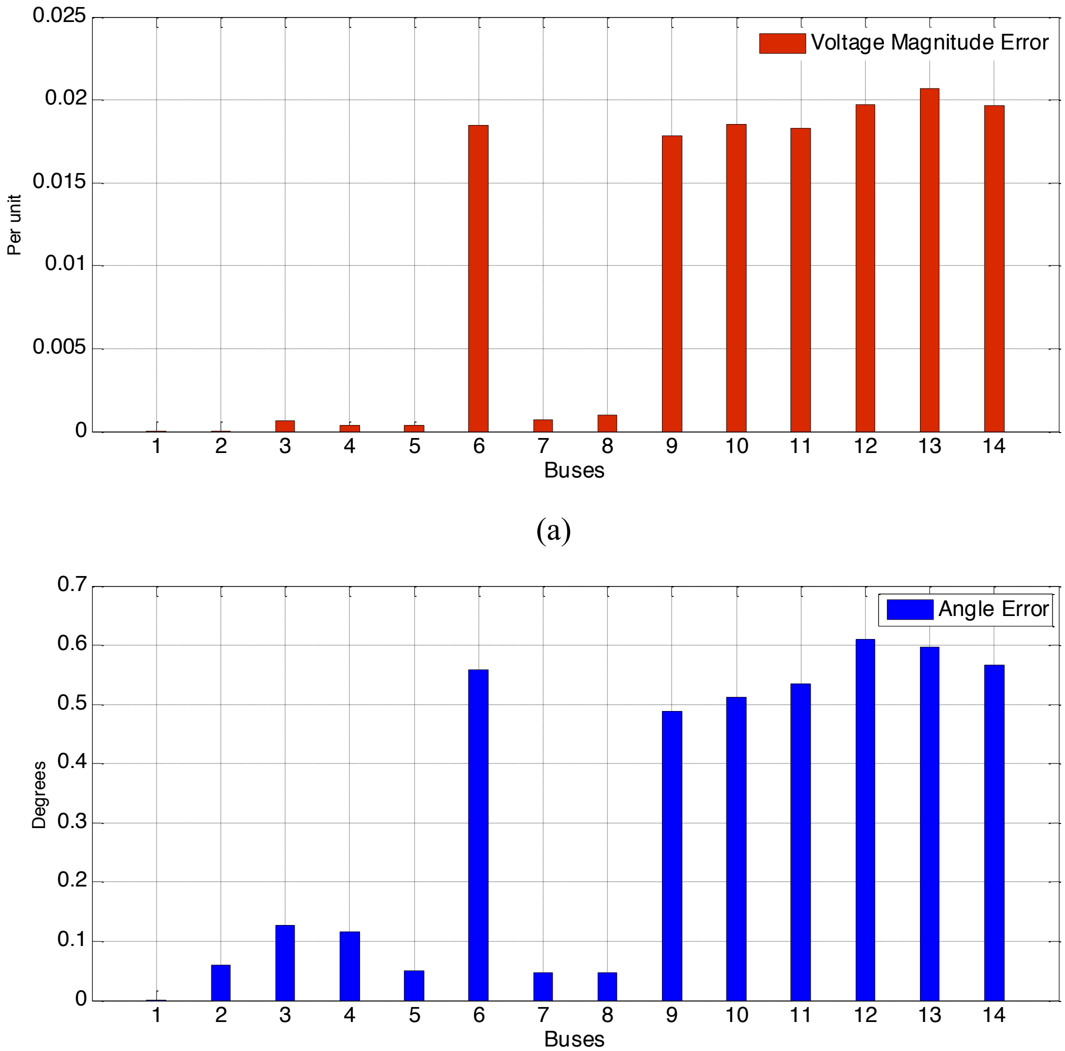

(a)

(b)

Figure 5.8: Voltage magnitude and phase angle errors in each bus

Next, critical measurements were identified from the properties of the covariance matrix of the residuals. The list of critical measurements are shown in Table 5.7, and the corresponding LNRT values are outlined in Table 5.8. Bad data were then injected into active power flow from Bus 4 to Bus 7, to verify whether the LNRT could detect it. The resultant residuals are shown in Table 5.9. The largest normalized residual was 0.583 for both Table 5.8 and 5.9. This is below the threshold value, and therefore the injected bad data could not be detected. More importantly, the occurrence of bad data within critical measurements caused the LNRT to fail to track the exact location of the bad data injection. The corresponding V_MAPE and Ɵ_MAE were calculated as 0.015 and 1.38, respectively. Here, the Ɵ_MAE increased significantly due to the occurrence of the bad data at the critical node in active power flow. This was reflected in each bus as shown in Fig. 5.9.

Table 5.8: Normalized Residual rN without bad data

Number	Measurement Type	rNconv (Without bad data)
1	P2-3	0.58
2	P1-2	0.57
3	P2	0.55
4	P2-5	0.55
5	P4	0.27

Table 5.9: Normalized Residual rN with bad data on P4-7

Number	Measurement Type	rNconv (With bad data)
1	Q12-23	0.58
2	P4	0.57
3	P10	0.55
4	P11	0.55
5	Q4	0.27

Table 5.10: PMU locations and mean errors of estimated states

Case	PMUs at Bus	V_MAE	Ɵ_MAE
1	No PMUs	0.0097	0.308
2	4,7,14	$4.23*10^{-4}$	0.040
3	**8,10,14**	**$2.84*10^{-4}$**	**0.023**
4	4,11,14	$3.84*10^{-4}$	0.027

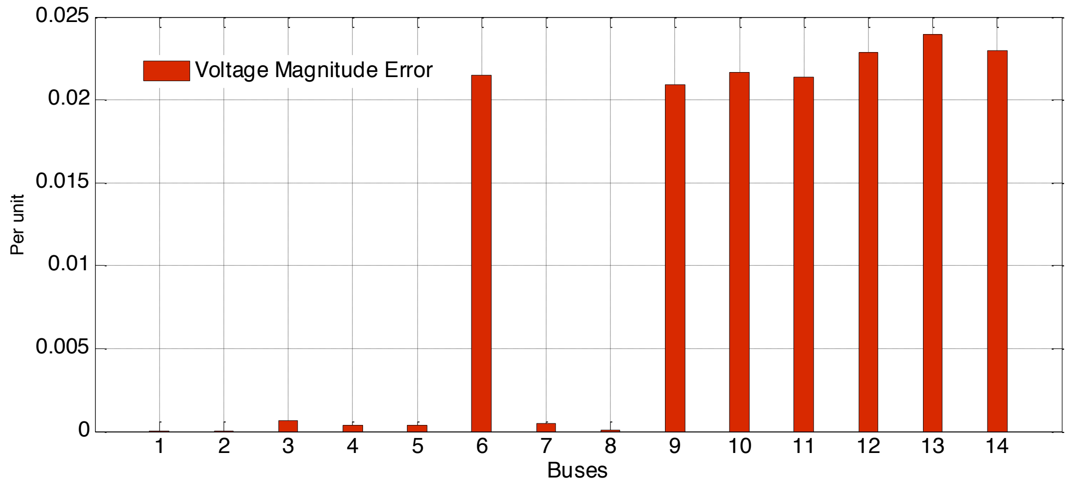

(a)

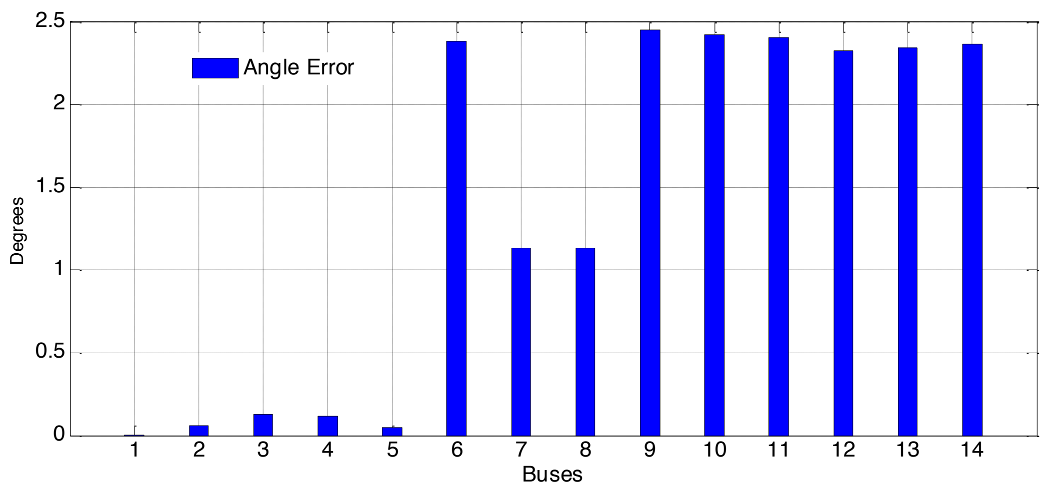

(b)

Figure 5.9: Voltage magnitude and phase angle errors in each bus with bad data on critical measurement

Finally, the inclusion of PMU measurements in the post-processing step to enhance bad data detection at critical locations was investigated. PMUs were strategically placed such that:

- They add redundancy and eliminate critical measurements and
- Improve the state estimation results

The number of PMUs required to eliminate all critical measurements in the grid was heuristically found to be three. Accordingly, Table 5.10 shows three combinations that were able to fulfill the above two conditions. Among the results, Case 3 provided the best estimation accuracy, giving a V_MAE of 2.84×10^{-4} and a Θ_MAE of 0.02. This can also be observed in the state estimation errors in each bus as illustrated in Fig. 5.10.

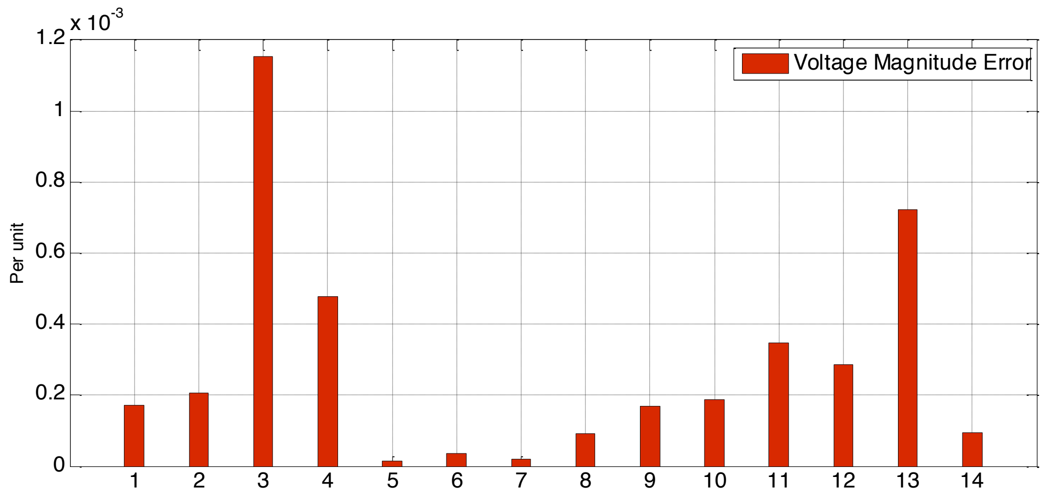

(a)

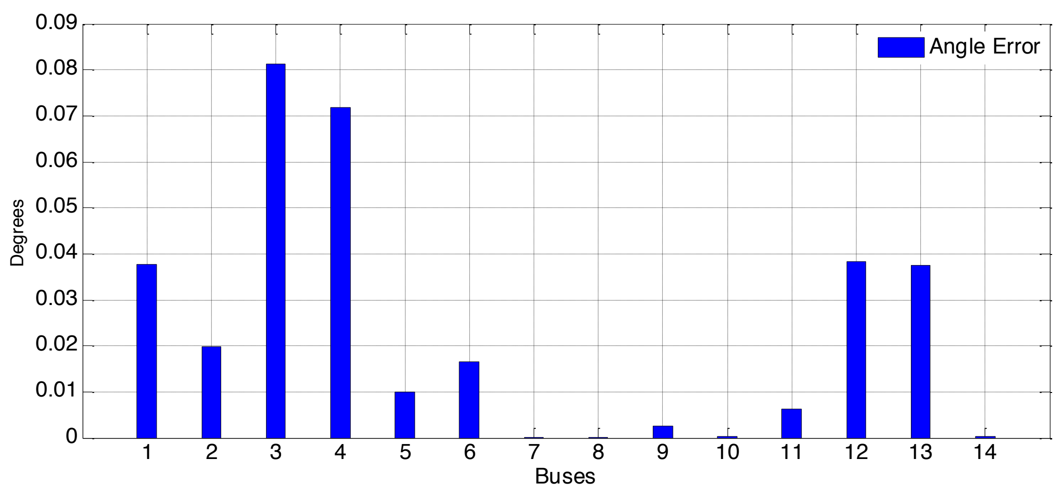

(a)

Figure 5.10: Voltage magnitude and phase angle errors in each bus with PMU measurements (Case 3)

In addition, Table 5.11 shows the new 5 largest normalized residuals that were obtained under the same bad data injection condition as of Case 1. The results showed that the largest normalized residual was 10.66, which was much larger than the detection threshold. In addition, the largest residual was computed at the location where bad data were injected. Thus, bad data in P4-7 could be correctly identified. The proposed integration of PMU measurements demonstrated to be an effective way to address bad data at critical locations. Subsequently, the estimated states of the grid could be further enhanced.

Table 5.11: Normalized Residual rN_new with BD on P4-7

Number	**Measurement Type**	**rN_{new}**
1	**P4-7**	**10.66**
2	Θ1	10.64
3	P4	6.48
4	P2-5	4.74
5	P2-4	2.99

CHAPTER 6

Conclusions and Future Work

State estimation is one of the most important Energy Management System applications in system operations. Its accuracy and operational robustness could potentially be further improved by utilizing PMU measurements. In this thesis a WLS based state estimator was developed and compared with IEKF based estimator. IEKF is a recursive algorithm that is more complex than WLS, which basically estimates based on taking a snapshot of the system at a particular time. The results of the comparison showed that WLS was more accurate since it has no process noise associated with the approximations introduced into the linearization of the process. However, IEKF was able to provide a prediction of the system states one-step ahead.

Bad data detection based on LNRT was integrated into the WLS estimator and a detailed analysis of its detection threshold was conducted. The results demonstrated the variability of the detection threshold with redundancy ratio proving against fixing the threshold. This test was conducted to understand the detection threshold variability and it is difficult to draw the mathematical relationship of the threshold using this method. Finally, this thesis showed that combining PMU measurements with existing RTU measurements enhanced the bad data detection capability of LNRT. This improved the overall accuracy of the existing state estimator without the need to modify the existing platform. They were added as a linear post-processing step and significantly improved the robustness of bad data detection capability. However, the placement of the PMUs should be in such a way that all critical measurements are eliminated. Otherwise, the LNRT could not be able to detect and identify bad data occurrence in such measurements.

Optimal PMU placement problem was not the scope of this thesis. Nevertheless, it is considered as part of the future work. Moreover, the identification of critical measurements from the residual covariance matrix was not reliable and therefore, a more reliable technique to identify critical measurements should also be developed.

Appendix

Test System Data

Appendix I: Bus Data of IEEE 14 Bus Test System

Bus no.	Bus Type	B	V	Angle
1	1	0	1.06	0
2	2	0	1.045	-4.98
3	2	0	1.01	-12.72
4	3	0	1.0186	-10.32
5	3	0	1.0203	-8.78
6	2	0	1.07	-14.22
7	3	0	1.062	-13.37
8	2	0	1.09	-13.37
9	3	0.19	1.0563	-14.95
10	3	0	1.0513	-15.1
11	3	0	1.0571	-14.79
12	3	0	1.0552	-15.08
13	3	0	1.0505	-15.16
14	3	0	1.0358	-16.04

Type: 1 slack, 2 PV, 3 PQ

Appendix II: Line Data of IEEE 14 Bus Test System

From Bus	To Bus	R (p.u)	X (p.u)	B/2 (p.u)	Transformer Tap (a)
1	2	0.01938	0.05917	0.0264	1
1	5	0.05403	0.22304	0.0246	1
2	3	0.04699	0.19797	0.0219	1
2	4	0.05811	0.17632	0.0187	1
2	5	0.05695	0.17388	0.017	1
3	4	0.06701	0.17103	0.0173	1
4	5	0.01335	0.04211	0.0064	1
4	7	0	0.20912	0	0.978
4	9	0	0.55618	0	0.969
5	6	0	0.25202	0	0.932
6	11	0.09498	0.1989	0	1
6	12	0.12291	0.25581	0	1
6	13	0.06615	0.13027	0	1
7	8	0	0.17615	0	1
7	9	0	0.11001	0	1
9	10	0.03181	0.0845	0	1
9	14	0.12711	0.27038	0	1
10	11	0.08205	0.19207	0	1
12	13	0.22092	0.19988	0	1
13	14	0.17093	0.34802	0	1

Bibliography

[1] F. C. Schweppe, "Power system static-state estimation, Part III: Implementation," *Power Apparatus and Systems, IEEE Transactions on,* pp. 130-135, 1970.

[2] F. C. Schweppe and D. B. Rom, "Power system static-state estimation, Part II: Approximate model," *power apparatus and systems, IEEE transactions on,* pp. 125-130, 1970.

[3] F. C. Schweppe and J. Wildes, "Power System Static-State Estimation, Part I: Exact Model," *Power Apparatus and Systems, IEEE Transactions on,* vol. PAS-89, pp. 120-125, 1970.

[4] F. F. Wu, "Power system state estimation: a survey," *International Journal of Electrical Power & Energy Systems,* vol. 12, pp. 80-87, 1990.

[5] A. Monticelli, "Electric power system state estimation," *Proceedings of the IEEE,* vol. 88, pp. 262-282, 2000.

[6] Y.-F. Huang, S. Werner, J. Huang, N. Kashyap, and V. Gupta, "State estimation in electric power grids: Meeting new challenges presented by the requirements of the future grid," *Signal Processing Magazine, IEEE,* vol. 29, pp. 33-43, 2012.

[7] R. Rajeev Kumar, M. Dewal, and K. Saini, "Utility of SCADA in power generation and distribution system," in *Computer Science and Information Technology (ICCSIT), 2010 3rd IEEE International Conference on*, 2010, pp. 648-652.

[8] N. Shivakumar and A. Jain, "A review of power system dynamic state estimation techniques," in *Power System Technology and IEEE Power India Conference, 2008. POWERCON 2008. Joint International Conference on*, 2008, pp. 1-6.

[9] W.-g. Li, J. Li, A. Gao, and J.-h. Yang, "Review and Research Trends on State Estimation of Electrical Power Systems," in *Power and Energy Engineering Conference (APPEEC), 2011 Asia-Pacific*, 2011, pp. 1-4.

[10] A. Leite da Silva and D. Falcao, "Bibliography on power system state estimation (1968-1989)," *Power Systems, IEEE Transactions on,* vol. 5, pp. 950-961, 1990.

[11] A. Gómez-Expósito, A. de la Villa Jaén, C. Gómez-Quiles, P. Rousseaux, and T. Van Cutsem, "A taxonomy of multi-area state estimation methods," *Electric Power Systems Research,* vol. 81, pp. 1060-1069, 2011.

[12] A. Garcia, A. Monticelli, and P. Abreu, "Fast decoupled state estimation and bad data processing," *Power Apparatus and Systems, IEEE Transactions on,* pp. 1645-1652, 1979.

[13] A. Monticelli, "Fast Decoupled State Estimator," in *State Estimation in Electric Power Systems*, ed: Springer, 1999, pp. 313-342.

[14] M. C. de Almeida, A. V. Garcia, and E. N. Asada, "Regularized least squares power system state estimation," *Power Systems, IEEE Transactions on,* vol. 27, pp. 290-297, 2012.

[15] A. Simoes-Costa and V. Quintana, "An orthogonal row processing algorithm for power system sequential state estimation," *Power Apparatus and Systems, IEEE Transactions on,* pp. 3791-3800, 1981.

[16] A. Abur and M. K. Celik, "Least absolute value state estimation with equality and inequality constraints," *Power Systems, IEEE Transactions on,* vol. 8, pp. 680-686, 1993.

[17] M. K. Celik and A. Abur, "A robust WLAV state estimator using transformations," *Power Systems, IEEE Transactions on,* vol. 7, pp. 106-113, 1992.

[18] A. S. Debs and R. Larson, "A dynamic estimator for tracking the state of a power system," *Power Apparatus and Systems, IEEE Transactions on,* pp. 1670-1678, 1970.

[19] D. Falcao, P. Cooke, and A. Brameller, "Power system tracking state estimation and bad data processing," *Power Apparatus and Systems, IEEE Transactions on,* pp. 325-333, 1982.

[20] A. Jain and N. Shivakumar, "Power system tracking and dynamic state estimation," in *Power Systems Conference and Exposition, 2009. PSCE'09. IEEE/PES*, 2009, pp. 1-8.

[21] M. Zima-Bockarjova, M. Zima, and G. Andersson, "Analysis of the state estimation performance in transient conditions," *IEEE Transactions on Power Systems,* vol. 26, pp. 1866-1874, 2011.

[22] T. Zhai, H. Ruan, and E. E. Yaz, "Performance evaluation of extended Kalman filter based state estimation for first order nonlinear dynamic systems," in *Decision and Control, 2003. Proceedings. 42nd IEEE Conference on*, 2003, pp. 1386-1391.

[23] G. Valverde and V. Terzija, "Unscented Kalman filter for power system dynamic state estimation," *IET generation, transmission & distribution,* vol. 5, pp. 29-37, 2011.

[24] M. Brown Do Coutto Filho and J. S. de Souza, "Forecasting-aided state estimation—Part I: Panorama," *Power Systems, IEEE Transactions on,* vol. 24, pp. 1667-1677, 2009.

[25] A. Sinha and J. Mondal, "Dynamic state estimator using ANN based bus load prediction," *Power Systems, IEEE Transactions on,* vol. 14, pp. 1219-1225, 1999.

[26] J.-M. Lin, S.-J. Huang, and K.-R. Shih, "Application of sliding surface-enhanced fuzzy control for dynamic state estimation of a power system," *Power Systems, IEEE Transactions on,* vol. 18, pp. 570-577, 2003.

[27] A. Abur and A. G. Exposito, *Power system state estimation: theory and implementation*: CRC Press, 2004.

[28] M. Zhou, V. A. Centeno, J. S. Thorp, and A. G. Phadke, "An alternative for including phasor measurements in state estimators," *Power Systems, IEEE Transactions on,* vol. 21, pp. 1930-1937, 2006.

[29] E. Blood, B. Krogh, and M. Ilic, "Electric power system static state estimation through Kalman filtering and load forecasting," in *Power and Energy Society General Meeting-Conversion and Delivery of Electrical Energy in the 21st Century, 2008 IEEE*, 2008, pp. 1-6.

[30] E. Blood, M. Ilic, and B. Krogh, "A Kalman filter approach to quasi-static state estimation in electric power systems," in *Power Symposium, 2006. NAPS 2006. 38th North American*, 2006, pp. 417-422.

[31] S. Sarri, M. Paolone, R. Cherkaoui, A. Borghetti, F. Napolitano, and C. A. Nucci, "State estimation of active distribution networks: comparison between WLS and iterated Kalman-filter algorithm integrating PMUs," in *Innovative Smart Grid Technologies (ISGT Europe), 2012 3rd IEEE PES International Conference and Exhibition on*, 2012, pp. 1-8.

[32] K. A. Clements, "Observability methods and optimal meter placement," *International Journal of Electrical Power & Energy Systems,* vol. 12, pp. 88-93, 1990.

[33] A. Expsito and A. Abur, "Generalized observability analysis and measurement classification," in *Power Industry Computer Applications., 1997. 20th International Conference on*, 1997, pp. 97-103.

[34] F. F. Wu and A. Monticelli, "Network observability: theory," *IEEE transactions on power Apparatus and Systems,* pp. 1042-1048, 1985.

[35] K. Clanents, G. Krutnpholz, and P. Davis, "Power system state estimation with measurement deficiency: an observability/measurement placement algorithm," *Power Apparatus and Systems, IEEE Transactions on,* pp. 2012-2020, 1983.

[36] A. Abur and A. G. Expósito, "Algorithm for determining phase-angle observability in the presence of line-current-magnitude measurements," *IEE Proceedings-Generation, Transmission and Distribution,* vol. 142, pp. 453-458, 1995.

[37] A. Jain, R. Balasubramanian, S. Tripathy, B. N. Singh, and Y. Kawazoe, "Power system topological observability analysis using artificial neural networks," in *Power Engineering Society General Meeting, 2005. IEEE*, 2005, pp. 497-502.

[38] E. Handschin, F. Schweppe, J. Kohlas, and A. Fiechter, "Bad data analysis for power system state estimation," *Power Apparatus and Systems, IEEE Transactions on,* vol. 94, pp. 329-337, 1975.

[39] H. M. Merrill and F. C. Schweppe, "Bad data suppression in power system static state estimation," *Power Apparatus and Systems, IEEE Transactions on,* pp. 2718-2725, 1971.

[40] J. Chen and A. Abur, "Placement of PMUs to enable bad data detection in state estimation," *Power Systems, IEEE Transactions on,* vol. 21, pp. 1608-1615, 2006.

[41] T. Van Cutsem, M. Ribbens-Pavella, and L. Mili, "Hypothesis testing identification: a new method for bad data analysis in power system state estimation," *Power Apparatus and Systems, IEEE Transactions on,* pp. 3239-3252, 1984.

[42] D. Elizondo, R. M. Gardner, and R. Leon, "Synchrophasor technology: The boom of investments and information flow from North America to Latin America," in *Power and Energy Society General Meeting, 2012 IEEE*, 2012, pp. 1-6.

[43] J. De La Ree, V. Centeno, J. S. Thorp, and A. G. Phadke, "Synchronized phasor measurement applications in power systems," *Smart Grid, IEEE Transactions on,* vol. 1, pp. 20-27, 2010.

[44] A. G. Phadke and J. S. Thorp, *Synchronized phasor measurements and their applications*: Springer Science & Business Media, 2008.

[45] A. Phadke, "Synchronized phasor measurements in power systems," *Computer Applications in Power, IEEE,* vol. 6, pp. 10-15, 1993.

[46] A. G. Phadke, "Synchronized phasor measurements-a historical overview," in *Transmission and Distribution Conference and Exhibition 2002: Asia Pacific. IEEE/PES*, 2002, pp. 476-479.

[47] J. Thorp, A. Phadke, and K. Karimi, "Real time voltage-phasor measurement for static state estimation," *Power Apparatus and Systems, IEEE Transactions on,* pp. 3098-3106, 1985.

[48] A. Gomez-Exposito, A. Abur, P. Rousseaux, A. de la Villa Jaen, and C. Gomez-Quiles, "On the use of PMUs in power system state estimation," in *Proc. 17th Power Systems Computation Conference*, 2011, p. 26.

[49] R. Zivanovic and C. Cairns, "Implementation of PMU technology in state estimation: an overview," in *AFRICON, 1996., IEEE AFRICON 4th*, 1996, pp. 1006-1011.

[50] B. Xu and A. Abur, "Observability analysis and measurement placement for systems with PMUs," in *IEEE PES power systems conference and exposition*, 2004, pp. 943-946.

[51] S. Chakrabarti and E. Kyriakides, "Optimal placement of phasor measurement units for power system observability," *Power Systems, IEEE Transactions on,* vol. 23, pp. 1433-1440, 2008.

[52] J. Peng, Y. Sun, and H. Wang, "Optimal PMU placement for full network observability using Tabu search algorithm," *International Journal of Electrical Power & Energy Systems,* vol. 28, pp. 223-231, 2006.

[53] R. F. Nuqui and A. G. Phadke, "Phasor measurement unit placement techniques for complete and incomplete observability," *Power Delivery, IEEE Transactions on,* vol. 20, pp. 2381-2388, 2005.

[54] S. Chakrabarti, E. Kyriakides, and D. G. Eliades, "Placement of synchronized measurements for power system observability," *Power Delivery, IEEE Transactions on,* vol. 24, pp. 12-19, 2009.

[55] Z. Hong-Shan, L. Ying, M. Zeng-Qiang, and Y. Lei, "Sensitivity constrained PMU placement for complete observability of power systems," in *Transmission and Distribution Conference and Exhibition: Asia and Pacific, 2005 IEEE/PES*, 2005, pp. 1-5.

[56] K.-P. Lien, C.-W. Liu, C.-S. Yu, and J.-A. Jiang, "Transmission network fault location observability with minimal PMU placement," *Power Delivery, IEEE Transactions on,* vol. 21, pp. 1128-1136, 2006.

[57] J. Zhu and A. Abur, "Bad data identification when using phasor measurements," in *Power Tech, 2007 IEEE Lausanne*, 2007, pp. 1676-1681.

[58] J. Chen and A. Abur, "Improved bad data processing via strategic placement of PMUs," in *Power Engineering Society General Meeting, 2005. IEEE*, 2005, pp. 509-513.

[59] G. N. Korres and N. M. Manousakis, "State estimation and bad data processing for systems including PMU and SCADA measurements," *Electric Power Systems Research,* vol. 81, pp. 1514-1524, 2011.

[60] B. Gou, "Generalized integer linear programming formulation for optimal PMU placement," *Power Systems, IEEE Transactions on,* vol. 23, pp. 1099-1104, 2008.

[61] J. Zhu and A. Abur, "Effect of phasor measurements on the choice of reference bus for state estimation," in *Power Engineering Society General Meeting, 2007. IEEE*, 2007, pp. 1-5.

[62] N. Balu, T. Bertram, A. Bose, V. Brandwajn, G. Cauley, D. Curtice*, et al.*, "On-line power system security analysis," *Proceedings of the IEEE,* vol. 80, pp. 262-282, 1992.

[63] J. D. Glover, M. Sarma, and T. Overbye, *Power System Analysis & Design, SI Version*: Cengage Learning, 2011.

[64] A. Tarali and A. Abur, "Bad data detection in two-stage state estimation using phasor measurements," in *Innovative Smart Grid Technologies (ISGT Europe), 2012 3rd IEEE PES International Conference and Exhibition on*, 2012, pp. 1-8.

[65] A. Abur, "Impact of phasor measurements on state estimation," in *Electrical and Electronics Engineering, 2009. ELECO 2009. International Conference on*, 2009, pp. I-3-I-7.